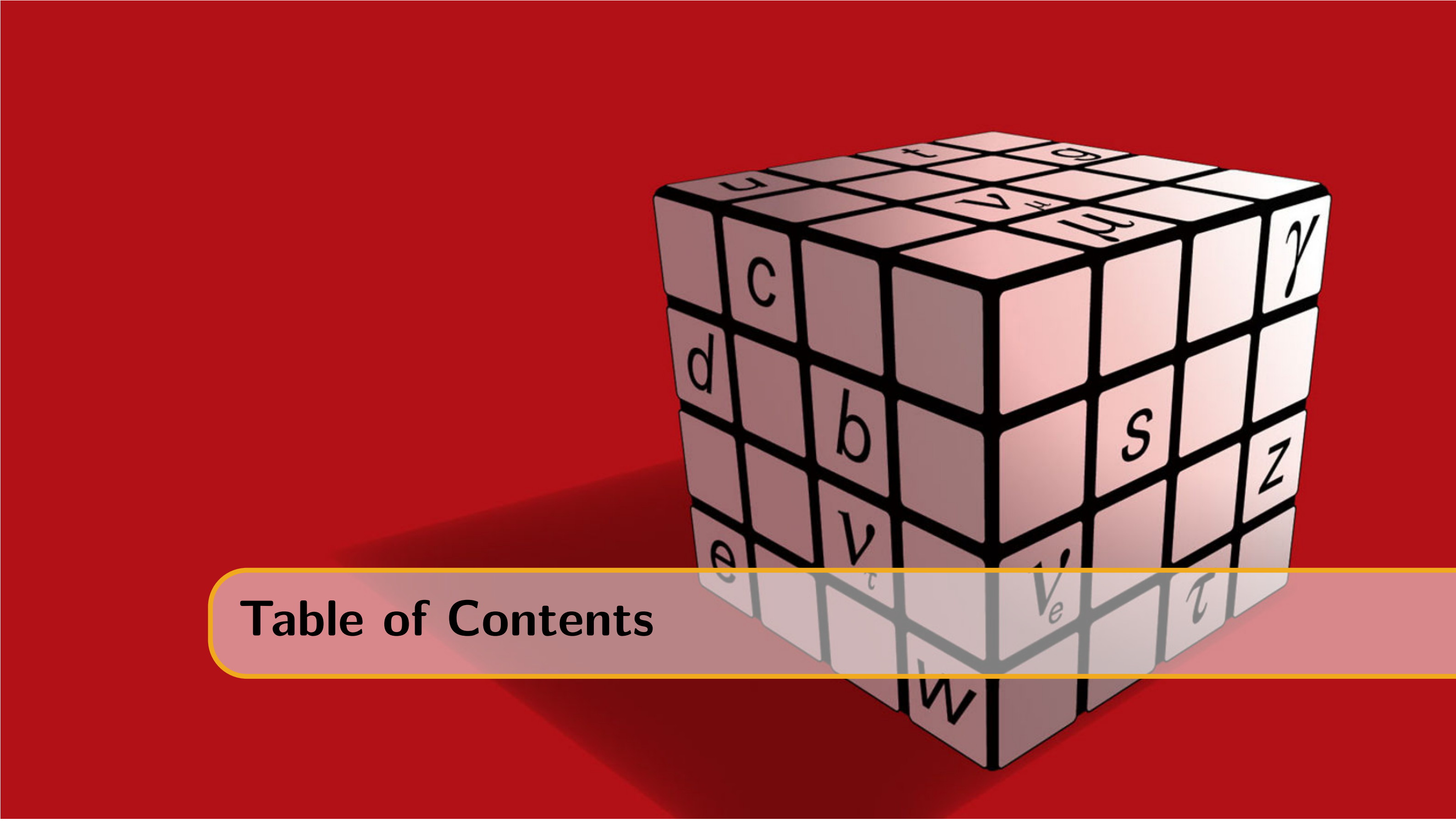

Table of Contents

III Additions

Theory and Experiment

II Simulation, Processing and Analysis

1. Simulation: Event Generation and Propagation

Soon there will be virtual reality, and augmented reality. If you assume any rate of improvement at all, then games will become indistinguishable from reality . . ., it would seem to follow that the odds we are in base reality are one in billions. ∼ *Elon Musk*

To be able to search for new physics, one has to have a good handle on the detector response on known physics processes. Depending on the analysis, some processes are more interesting than others. In general, the particle interactions of interest are referred to as *signal events*. Other interactions, which mimic or obscure the signal events, are typically called *background events*. These events are simulated using Monte Carlo[*] (MC) simulations, where one makes use of a model that describes the interactions and their probability to occur. A typical MC simulation consists of hundreds to millions of events that are constructed using these models with the use of random number generators. To determine the detector response of a particle interaction, one first has to start with the particle generation, which sets the conditions of the initial interaction. Afterwards, the propagation of the particle in the detector (medium) is simulated as best as possible. Below, we give an overview of the important background and signal simulations that are used in this analysis. A flowchart of the simulations steps is given in Fig. 1.1.

Corollary 1.0.1 — The software framework. *IceTray* is a modular framework written and used by the IceCube collaboration and mostly written in C++ for fast computation. A python interface for most modules is provided for fast and easy implementation of the code. The framework is used in both online and offline processing and is stream-based with modules that act on events in the stream and essentially follows a flowchart of modules that is provided by the user.

To process the large amount of simulation that is required for the collaboration, a data processing and management framework called *IceProd* was developed. The setup is very light-weight, running as a python application. It uses (complex) workflow DAGs (see below) across distributed computing grids in order to optimize usage of resources. A *dataset* is set

[*]While recovering from an illness in 1946, Stanislaw Ulam figured that the actual counting of succesful attempts in playing a card game would yield him a much faster answer to the probability of succes rather than doing the actual calculus. His work, shared with John von Neumann, needed to remain secret and adopted the code word "Monte Carlo", referring to the gambling games in the Monte Carlo Casino in Monaco.

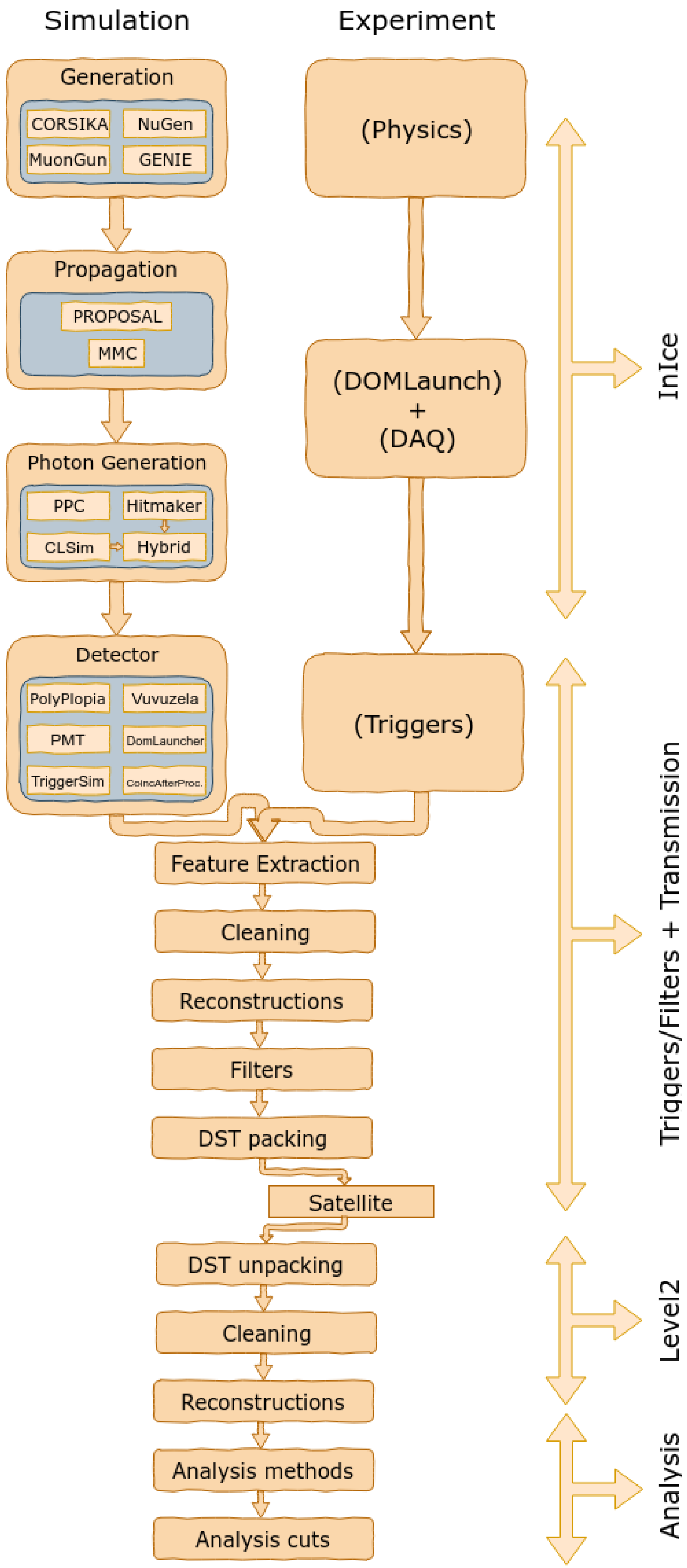

Figure 1.1: Flowchart of the simulation layout. On the left is shown that particles are injected and their interactions are simulated to digitized waveforms. The right part shows real data processing. After triggering both data and simulation go through the same processing chain to prepare for analysis.

up by running hundreds to thousands of jobs in parallel over multiple computing resources all over the world. Each dataset has specific input parameters that are fixed. Distributions in physical parameters such as the direction, energy, position, etc. of the particle(s) are provided by random number generators [179].

HTCondor is an open source computing software that provides a job queueing mechanism, scheduling policy, priority scheme, resource monitoring, and resource management. Users submit their serial or parallel jobs to HTCondor and places them into a queue. It chooses when and where to run the jobs based upon a policy, carefully monitors their progress, and ultimately informs the user upon completion.

DAGMans (Directed Acyclic Graph Managers) are meta-schedulers for the execution of computations. They submit the programs to HTCondor in an order that is represented by a DAG and processes the results. DAGMans are often used by analyzers for bulk computations on large amounts of data.

1.1 Generation

Simulations start with setting up the starting conditions of the physical processes one wants to simulate. For example, a shower event by itself is not well defined. The type of primary particle (H, He, Fe,...), the energy, the inclination and so on will all define the properties of the full air shower that will be produced. Multiple different generators used in the IceCube collaboration serve other purposes; some are explained in more detail below.

1.1.1 Background simulation

1.1.1.1 CORSIKA

A free, publicly available software framework that is widely used in the astrophysics community for the simulation of cosmic ray interactions is called CORSIKA (COsmic Ray SImulations for Kascade). It was originally developed for the KASCADE experiment and now used by most people and collaborations to simulate air shower events. IceCube analyses, such as this one, use CORSIKA simulations to simulate the muonic component that is able to reach the in-ice detector.

The code is written in FORTRAN 77, but a C++ version is currently in the making [181].

A particle of specific type, energy, direction and position is injected in the top of the atmosphere and propagated. The distribution of particles in the shower is saved and read out according to a certain altitude. Because the flux of cosmic rays is exceedingly small at the highest energies, too many resources and too much time would be required to simulate an energy distribution as measured in experiments. Therefore, one often simulates a much harder spectrum and reweights the events accordingly later on (see Section D.4). Simulation datasets are often subdivided into a low-energy and high-energy dataset. The former ranges from primary energies between 600 GeV to 100 TeV and uses a spectral index that is close to what is measured. The spectral index of the latter is smaller, resulting in a harder spectrum, and the primary energy ranges from 100 TeV to 100 EeV. The lower limit of the energy range is due to the limited penetration depth of muons through the ice. An overview is given in Table 1.2.

The spectrum used for this analysis, after reweighting, follows the following energy distribution:

$$\Phi_i\left(E_{\text{prim}}\right) = \sum_{j=1}^{3} a_{i,j} E^{-\gamma_{i,j}} \cdot \exp\left[-\frac{E}{Z_i R_{c,j}}\right]. \tag{1.1}$$

where we sum over the three populations that are mentioned in Section **??**, γ is the spectral index, Z the particle atomic number and $a_{i,j}$ the normalization constants for primary i in population j. The 5 groups that are assumed to contribute significantly to the flux are: p, He, CNO, Mg-Si

Table 1.1: Best fit for parameters in Eq. 1.1. Numbers taken from Ref. [94].

j	R_c [V]	γ					$a_{i,j}$				
		p	He	CNO	Mg-Si	Fe	p	He	CNO	Mg-Si	Fe
1	$4 \cdot 10^{15}$	1.66	1.58	1.63	1.67	1.63	7860	3550	2200	1430	2120
2	$30 \cdot 10^{15}$	1.4					20		13.4		
3	$2 \cdot 10^{18}$	1.4					1.7		1.14		

and Fe. This is the convention that is used in Ref. [94]. Table 1.1 shows the best fits for the normalization constants to describe the data.

Interactions

The atmosphere composition is always set at 78.1% N_2, 21% O_2, and 0.9% Ar, which is a good description of reality. However, the density of the air above the detector changes significantly during the year because of temperature differences in the Arctic Summer and Winter. Most analyses treat the muonic component as a background and are not interested in the details of the showers and how it changes during the year and therefore use an average of the atmospheric density.

The shower propagation and composition depends on the models that are used to simulate these high-energy interactions. The lowest energies are simulated with FLUKA (FLUktuierende KAskade) [180]. This model covers the energy range that can be compared with accelerator experiments. Which model is the best for the highest energies is not known at the time of writing since there are no controlled laboratory measurements that are capable of reaching these energies. Several studies seem to indicate that the composition changes drastically at the highest energies SAMCITEREN+andere. Fortunately, this is of no importance for this analysis.

1.1.1.2 NuGen

The neutrino-generator (NuGen) is a neutrino event generator program that works with the IceTray framework. With this module, one can inject a primary neutrino on the surface of the Earth by specifying a few parameters in the steering file.

The physics implemented in this program is based on the ANIS-All Neutrino Interaction Generator [182]. However, the cross sections have been updated and the structure of the code has been changed significantly from ANIS to incorporate it in the IceTray framework.

The generator requires the first interaction to be near the detector and

- prepares a primary neutrino and injects it to the Earth,
- propagates the neutrino and works out interactions inside the Earth* (when they occur),
- makes a forced interaction inside the detection volume† (only if any neutrino reaches the detector site),
- stores injected neutrinos and all generated secondaries,
- stores interaction weight information.

The generator also does not distinguish between neutrino and antineutrino and assumes a ratio of (1:1).

The spectrum used for this analysis, after reweighting, follows the Honda2006 spectrum [125] for atmospheric neutrinos, SarcevicStd for the prompt component [128], and an astrophysical flux fit

*Possible interactions are CC, NC, Glashow resonance for $\bar{\nu}_e$ and tau decay for $\overset{(-)}{\nu}_\tau$. CC interactions produces no new neutrinos and the simulation stops at the vertex point. The other interactions create new secondary neutrinos.

† In most cases, a neutrino will not interact within the medium, but for computational reasons at least one neutrino is forced to interact and the simulation is reweighted afterwards accordingly.

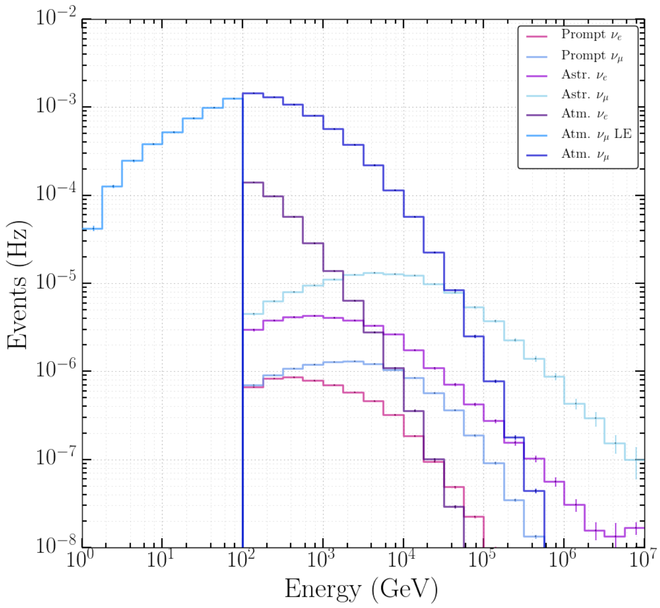

Figure 1.2: Distribution of weighted neutrino fluxes that were used for this analysis. The atmospheric ν_μ and ν_e fluxes were derived from Ref. [125], prompt from Ref. [128], and astrophysical from Ref. [183].

from Ref. [183] (see Section **??** for more information on these fluxes). The astrophysical flux measured by the IceCube collaboration follows an energy spectrum equal to

$$E^2 (\Phi) = 1.5 \cdot 10^{-8} \left(\frac{E}{100\ \text{TeV}} \right)^{-0.3} \text{GeV cm}^{-2}\text{s}^{-1}\text{sr}^{-1}. \tag{1.2}$$

The distribution for these different components can be seen in Fig. 1.2.

1.1.1.3 GENIE

To include the lowest energies, which are not accounted for by ANIS/NuGen, the GENIE (Generates Events for Neutrino Interaction Experiments) neutrino generator was implemented in IceTray. It is a well established generator, used by collaborations worldwide and written in C++ [184, 185].

The spectrum used for this analysis, after reweighting, follows the Honda2015 spectrum [186] for low-energy atmospheric neutrinos.

1.1.2 Signal simulation

As mentioned in Section **??**, the signal flux is assumed to be isotropic close to the detector. The SMP starting points are randomly placed on a disk with a direction perpendicular to it as shown in Fig. 1.3. The disk has a radius of 800 m and is located at a distance of 1000 m from the detector center. The disk itself is randomly rotated around the detector center to simulate an isotropic flux. The distribution of the azimuth, ϕ, and cosine of the zenith*, $\cos(\theta)$, is shown in Fig. 1.4.

Because slow moving particles would require specialized treatment, the minimal velocity of the particles is set as $\beta > 0.95$ and simulated with an E^{-1} spectrum. The spectrum is later normalized to a flux of 10^{-14} GeV cm^{-2} s^{-1} sr^{-1} with an E^{-2} spectrum (see Appendix D.2) where the absolute flux is only necessary for illustrative purposes, see Section refer to this section

*See Appendix D.3 why we show the cosine of the zenith.

Table 1.2: Overview of the datasets used in this analysis. GaisserH3a from Ref. [94], Honda2015 from Ref. [186], Honda2006 from Ref. [125], Sarcevic from Ref. [128], and astrophysical from Ref. [183].

Generator	Type	Range [GeV]	Simulated γ	Weighted γ	Ice	Dataset
CORS.	5-comp.	$10^5 - 10^{11}$	2	GaisserH3a	SpiceLea	11937
CORS.	5-comp.	$600 - 10^5$	2.6	GaisserH3a	SpiceLea	11499
CORS.	5-comp.	$600 - 10^5$	2.6	GaisserH3a	SpiceLea	11808
CORS.	5-comp.	$600 - 10^5$	2.6	GaisserH3a	SpiceLea	11865
CORS.	5-comp.	$600 - 10^5$	2.6	GaisserH3a	SpiceLea	11905
CORS.	5-comp.	$600 - 10^5$	2.6	GaisserH3a	SpiceLea	11926
CORS.	5-comp.	$600 - 10^5$	2.6	GaisserH3a	SpiceLea	11943
CORS.	5-comp.	$600 - 10^5$	2.6	GaisserH3a	SpiceLea	12161
CORS.	5-comp.	$600 - 10^5$	2.6	GaisserH3a	SpiceLea	12268
GENIE	ν_μ	$0.5 - 100$	1	Honda2015	SpiceMie	12475
NuGen	ν_μ	$100 - 10^8$	2	atmos.: Honda2006 prompt: Sarcevic astro.: Astro.	SpiceLea	11029
NuGen	ν_μ	$100 - 10^8$	2	atmos.: Honda2006 prompt: Sarcevic astro.: Astro.	SpiceLea	12346
NuGen	ν_μ	$100 - 10^8$	2	atmos.: Honda2006 prompt: Sarcevic astro.: Astro.	SpiceLea	11883
NuGen	ν_e	$100 - 10^8$	2	atmos.: Honda2006 prompt: Sarcevic astro.: Astro.	SpiceLea	12034
NuGen	ν_e	$100 - 10^8$	2	atmos.: Honda2006 prompt: Sarcevic astro.: Astro.	SpiceLea	12646

Table 1.3: Overview of the datasets used for systematic uncertainties. Polyg(onato) follows from Ref. [187], GaisserH4a from Ref. [188] and Bartol from Ref. [189].

Generator	Type	Range [GeV]	Sim. γ	Weighted γ	Ice	Dataset	Syst. Eff.
CORS.	Hoerandel	$600 - 10^5$	Polyg.	GaisserH3a	SpiceLea	11527	DOM eff. -10%
CORS.	Hoerandel	$600 - 10^{11}$	Polyg.	GaisserH3a	SpiceLea	11526	DOM eff. +10%
CORS.	5-comp.	$600 - 10^{11}$	2.6	GaisserH3a	SpiceLea	12388	Abs. +10% Scat. +10% Abs./Scat. -7.1%
CORS.	All datasets from Table 1.2			GaisserH4a	SpiceLea	Table 1.2	GaisserH4a
NuGen	ν_μ	$100 - 10^8$	2	Bartol (syst.)	SpiceLea	11029	Bartol flux
NuGen	ν_μ	$100 - 10^7$	2	Honda2006 + Bartol (syst.)	SpiceLea	11883	DOM eff. +10% DOM eff. -10% Abs. +10% Scat. +10% Abs./Scat. -7.1% Bartol flux
NuGen	ν_μ	$100 - 10^8$	2	Honda2006 + Bartol (syst.)	SpiceLea	12346	DOM eff. +10% DOM eff. -10% Abs./Scat. -7.1% Bartol flux

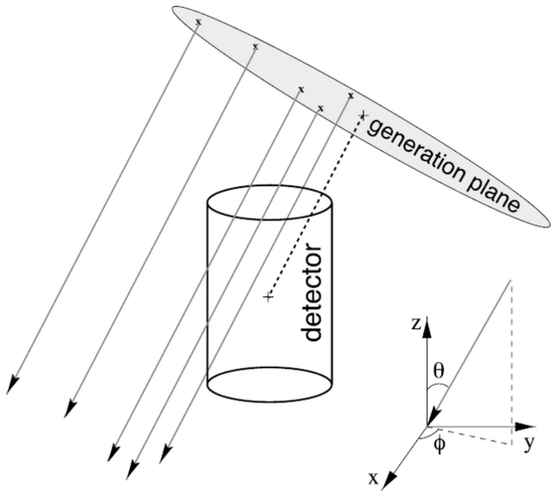

Figure 1.3: Illustration of how the particle injection works. The particle is first randomly positioned on a disk following a uniform distribution. The disk is then randomly rotated to simulate an isotropic flux.

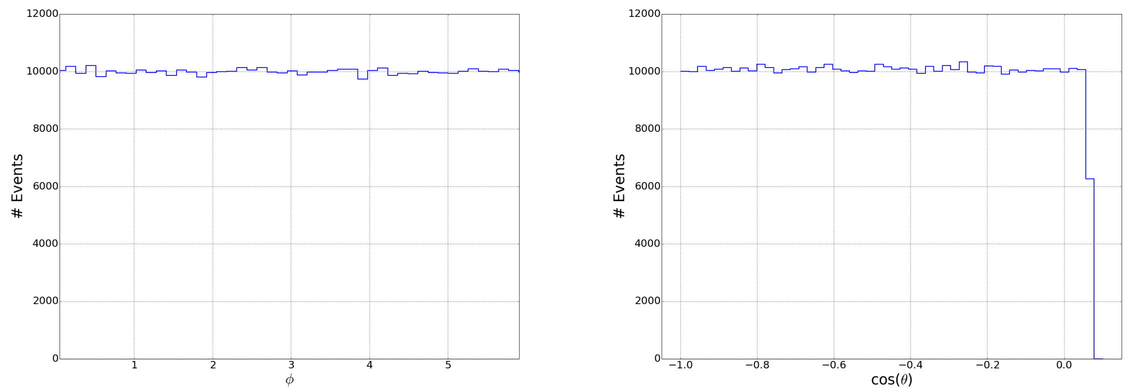

Figure 1.4: Illustration of uniform distributions of azimuth and cosine of the zenith for the particle injection in agreement with an isotropic flux (see Appendix D.1).

.

when it's written!.

Similar to the background, SpiceLea was used as the nominal ice model.

1.2 Propagation

After generation, the particles need to be propagated through the medium. The particles will interact, lose energy, produce new particles, and generate light. The particle interactions and light production are done in two different modules as photon simulation is done with GPU. The former module is called `PROPOSAL`, the latter `ppc`.

1.2.1 `PROPOSAL`

Using the cross sections of the important interaction, together with the properties of the traversing medium and the particles (mass, charge, spin, decay time, etc.) it is possible to simulate the energy losses, secondary production and the consequent interaction of these daughter particles. This is done in the software package `PROPOSAL` (the Propagator with Optimal Precision and Optimized Speed for All Leptons), fully written in C++. It was based on the former program `MMC` (Muon Monte Carlo), which was written in Java. In 2018, a substantial improved version of

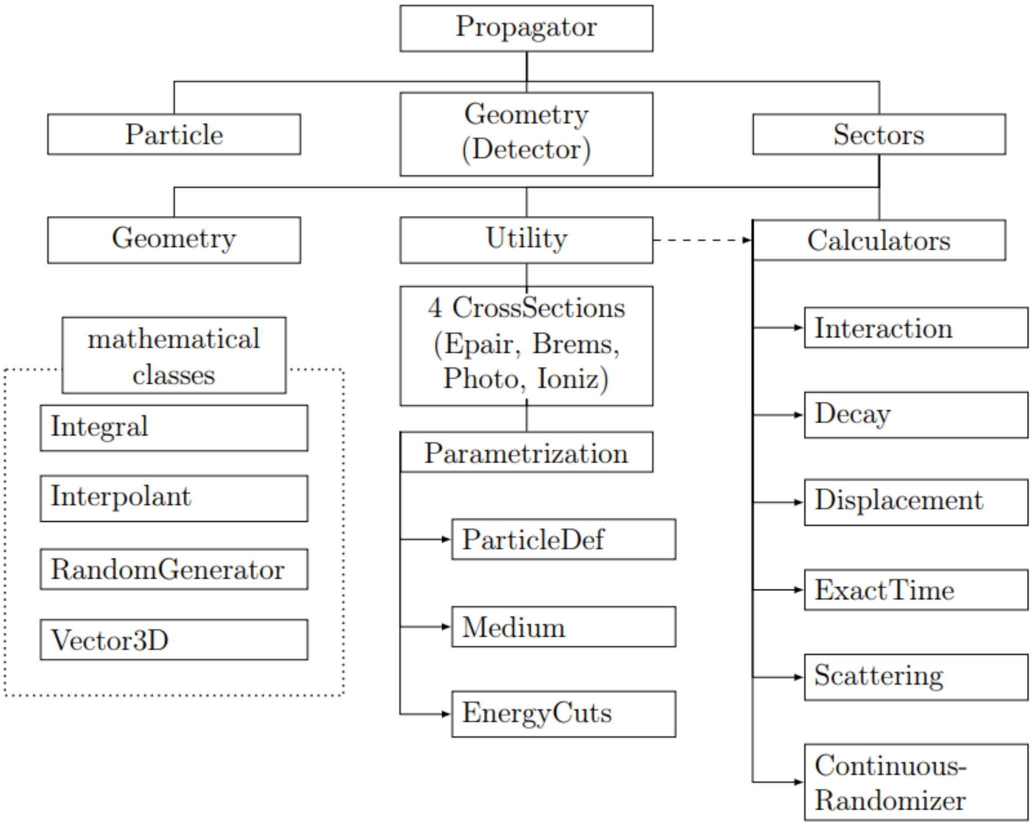

Figure 1.5: Overview of the class structure in `PROPOSAL`, from Ref. [190].

`PROPOSAL` was finalized. An illustration of the workings of the code is given in Fig. 1.5 and an in depth documentation is given in Ref. [190].

`PROPOSAL` for SMPs

Since we assume the SMPs to behave leptonically, it was chosen to use PROPOSAL for the signal propagation as well. The mass and charge of the particle are set in the input parameters and the cross section dependence on these parameters can be seen in Section **??**. In general, there is a small dependence on the mass and a squared dependency on the charge (Eq. ???), except for bremsstrahlung that has a quadratic charge dependency. These effects only become prominent and important for highly relativistic particles, which as will be seen in Section verwijs hiernaar als je dit geschreven hebt, do not have a dominating contribution to the total signal.

The `PROPOSAL` module keeps track of all the particles that are produced during propagation and the accompanying energy losses in a tree-like structure (called an *I3MCTree*). This collection of particles and their interactions are forwarded to a light production computation module.

1.2.2 Photoelectron generators

In Section **??** we already explained how the ice is simulated in the IceCube detector. The parameters $b_e(400)$ and $a_{dust}(400)$ define the photon propagation through the ice and determine if they are absorbed or hit a DOM. To optimize computing time, the DOMs were scaled (mostly with a factor of 5) to force more photon interactions. The number of photons emitted was then appropriately scaled down with the square of this scaling factor*. The DOM acceptance curves, as shown in Fig. **??**, together with the Frank-Tamm formula (Eq. **??**) allow to calculate the expected number of photons produced per unit length:

*The surface of a sphere scales with the square of the radius.

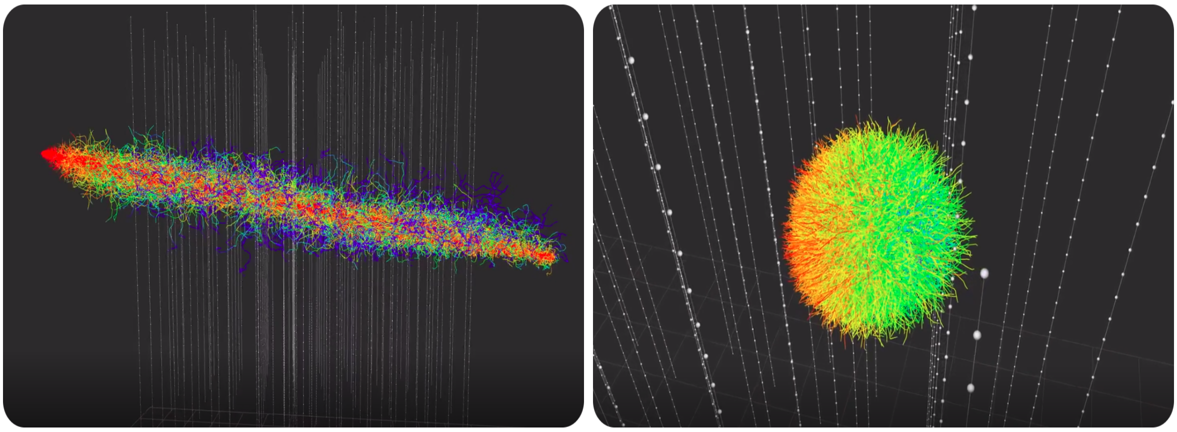

Figure 1.6: *Left:* simulation of a track event in IceCube. Each line represents a photon path and colors indicate how far they have traveled from their generation point. *Right:* simulation of a cascade event in IceCube.

$$\frac{dN}{dx} = \int_{\lambda_1}^{\lambda_2} \frac{2\pi\alpha}{\lambda^2} \sin^2(\theta_c)\, d\lambda = 2\pi\alpha \sin^2(\theta_c) \left(\frac{1}{\lambda_1} - \frac{1}{\lambda_2}\right). \tag{1.3}$$

From this formula, we find that the expected rate of a Cherenkov emission profile is equal to ≈ 350 photons/cm. Together with the DOM acceptance, which has an overall average of around 7%, the expected *seen* number of photons per meter is equal to 2450 m^{-1}.

`PPC` is a Photon Propagation Code, written in C++ and runs on graphic processing units (GPUs). This allows the code to run up to a hunderd times faster than in a CPU-only environment. `PPC` employs both CUDA (NVIDIA GPU only) and OpenCL programming interface (both NVIDIA and AMD GPUs) together with multiple CPU environments. GPU environments allow the tracking of thousands of photons simultaneously, vastly improving the computational speed. For more information, see Ref. [191].

Previous photon propagation code, such as `Photonics` [192], produced 6-dimensional photon tables (3 spatial, 2 directional and 1 temporal). This meant that at least one set of tables had to be produced per particle type and per velocity and interpolation methods had to be used, with the accompanying inaccuracies. These tables also required significant disk space and the method was therefore replaced with the GPU-codes. Direct photon simulation also allows for other non-trivial implementations such as the tilting of ice layers.

Another photon propagation code is called `CLSim`, which uses GEANT4 to propagate particles. A hybrid version called `HybridCLsim` is sometimes used. Muons are propagated using `PROPOSAL/MMC` and their stochastic losses (which are showers) are simulated from tables whereas the "bare muons" (with their stochastics) are simulated using direct propagation. This avoids time loss for the rare but very computational high-energy cascade events.

An illustration of photon propagation in the IceCube detector for both a cascade and track simulation is shown in Fig. 1.6.

1.3 Detector simulation

Further processing of the simulations involve:

- `Polyplopia`: a project dedicated to merge multiple events to account for coincident events (that are simulated independently). An estimated 15% of CORSIKA events result in coincident events and make up de bulk of bad reconstructions where down-going muons are simulated as up-going (example see Fig. **??**);

- `Vuvuzela`: the PMT noise is simulated as having an exponential component from thermal and radioactive decays, and a log-normal contribution for scintillation;
- `PMT`: the time from the first photon entering the PMT to the readout after passing along multiple dynodes has an uncertainty, referred to as "PMT jitter" . The amplification of photoelectrons by the PMT is also not constant and is simulated in this module. Additionally, the module accounts for prepulses, late pulses, afterpulses and saturation of the PMT. More information can be found in Refs. [144, 193].
- `DOMLauncher`: the digitization of the PMT pulses and other behavior of the DOM mainboard (as explained in Section **??**) is done in this module. The three main features of the DOM that are simulated to generate launches are the discriminator, LC, and digitization.
- `trigger-sim`: simulation of the trigger behavior as explained in Sec. **??**.

1.4 Burn sample

Getting the intricate details of physical events in non-trivial environments just right is not an easy task. In many steps of the way, simulations use fits and estimations. Some simulation datasets are reasonable to compare to the data, depending on the phase space one is looking at, while other datasets need other specifications. For example, analyses dedicated to measuring the cosmic ray interactions need much more fine-tuning in their models for the atmosphere, composition, interaction models, etc. than an analysis dedicated to search for muon tracks that first propagated through the Earth and have atmospheric muons as a background.

It is for this reason, most analyses select a certain subset of the data they want to analyze to compare to the Monte Carlo simulations. For this analysis, 10% of the total data, called the *burn sample* , was used to compare data to Monte Carlo. As indicated in Section **??**, the data is saved in 8-hour runs and the burn sample consists of every run ending with a '0'. The burn sample also allows to estimate the robustness of certain reconstructions and variables regarding differences in data and simulation.

More info on the burnsample see Section???

1.4.1 Standard ??

Processing ergens: online L0, L1, L2, uw filters,... Beter in analysis hoofdstuk?

1.5 Event viewer

After a full simulation, it is possible to visualize the event in an event viewer called `Steamshovel` . Typical events in the IceCube detector are shown with this interface and are loaded from *i3files* that contain information about the detector geometry and the full event (DOM positions and calibrations, detector hits, timestamps, trigger hits, etc.). Simulated events also contain the true values of the particles and can be compared with reconstructed variables. Event viewers allow for first guesses in how background events are able to be separated from signal, although both can have wide varieties in possible outputs.

The number of photons seen per DOM is indicated by the size of the spheres; the larger the sphere, the more PEs were seen. The color of the modules indicates the time of the pulse registration. The color scale can be chosen, but usually a rainbow pattern is used where red indicates the earliest pulse hits and blue the last.

An example is given in Fig. ??? wat is goed?

en in eerste steamshovel verwijzen naar dit deel?.

2. The SPACE Analysis

De uitleg van temperature modulations is goed in Sam zijn thesis https://arxiv.org/pdf/physics/0312102v1.pdf
https://arxiv.org/pdf/1310.1284.pdf

Ook ergens een tabel maken met info over je data runs. Duidelijk maken wat de livetime is bv en ook zeggen van wanneer to wanneer een bepaalde run liep (2011: mei 2011- mei 2012)

Klaus zijn paper? https://arxiv.org/abs/1806.05696

2.1 Motivation

2.2 General strategy

2.3 Event cleaning

2.4 Variables

2.5 BDT results

2.6 Pull validation

2.7 Systematic Uncertainties

2.8 Results

3. Summary and Discussion

III

Additions

Appendices

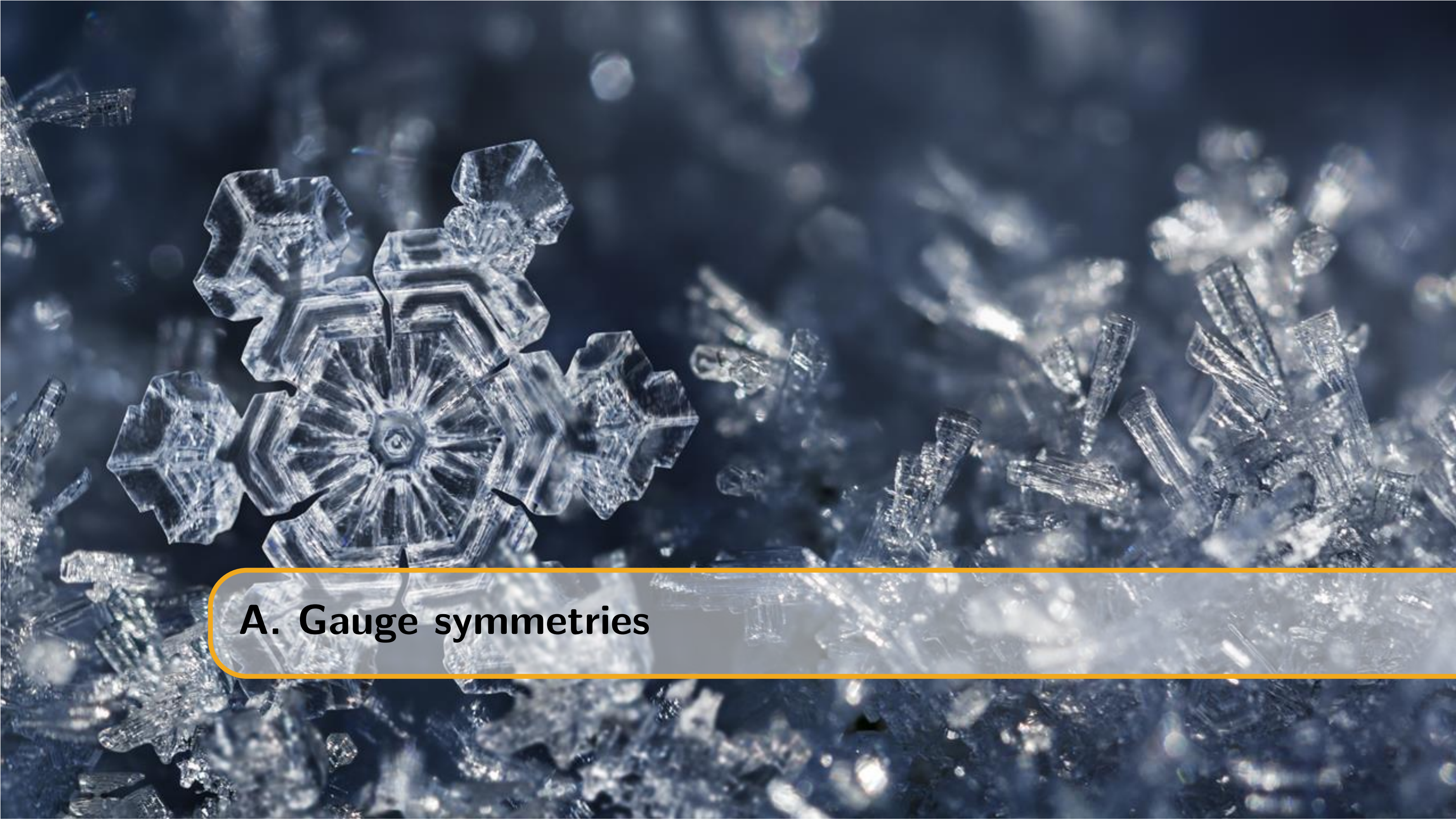

A. Gauge symmetries

NOG NIET GEDAAN

The difference between global and local symmetries are not straightforward for everybody. In this appendix I try to give a better view of the matter.

Imagine that at each point in space and time there is a circle attached to it. If one shifts all circles of all points with a fixed angle the underlying physics hasn't changed. If we look at the whole in a different angle, nothing seems to be changed as everything holds the same relative orientation. This is a global symmetry. For local symmeries we instead shift each circle through a different angle, but an angle that changes smoothly from point to point and in a way that we can say how that angle is varying between different nearby regions. Then it will turn out that we can describe that rotation angle by means of a so-called gauge field, which just lets us transport the charged scalar field from one point in space time to another, taking account of how the rotation angle of the circle is changing. A gauge is a kind of coordinate system that is varying depending on the location with respect to some underlying space. In physics we are almost always concerned with space-time as the underlying space, and we are typically interested in theories that are invariant with respect to the choice of gauge or coordinate system.

Dan wat uitleg vanuit je QFT boek en de dingen hieronder: Je wilt je derivative anders doen werken in je theory onder een transformatie, maar daarvoor heb je een veld nodig. M.a.w.: dankzij een veld heb je lokale ijktransformatie mogelijk!

B. Planck's law

bron: http://hyperphysics.phy-astr.gsu.edu/hbase/quantum/rayj.html

B.1 Electromagnetic waves in a cubical cavity

Suppose we have EM waves in a cavity at equilibrium with its surroundings. These waves must satisfy the wave equation in three dimensions:

$$\frac{\partial^2\Psi}{\partial x^2}+\frac{\partial^2\Psi}{\partial y^2}+\frac{\partial^2\Psi}{\partial z^2}=\frac{1}{c^2}\frac{\partial^2\Psi}{\partial t^2}. \tag{B.1}$$

The solution must give zero amplitude at the walls. A non-zero value would mean energy is dissipated through the walls which is in contradiction to our equilibrium assumption. A general solution takes the form of

$$\Psi(x,y,z,t)=\Psi_0\sin k_1x\sin k_2y\sin k_3z\sin k_4t, \tag{B.2}$$

which, after requiring $k_nL=n\pi$ with $n=0,1,2...$ and $k_4\frac{\lambda}{2c}=\pi$, leads to

$$\Psi(x,y,z,t)=\Psi_0\sin\left(\frac{n_1\pi x}{L}\right)\sin\left(\frac{n_2\pi y}{L}\right)\sin\left(\frac{n_3\pi z}{L}\right)\sin\left(\frac{2\pi ct}{\lambda}\right). \tag{B.3}$$

From the wave equation it is easy to find that

$$n^2=n_1^2+n_2^2+n_3^2=\frac{4L^2}{\lambda^2}, \tag{B.4}$$

which span up a sphere in "n-space" with a volume of $\frac{1}{8}\frac{4}{3}\pi n^{3/2}$, where the first term originates from the positive nature of $n_{1,2,3}$. Because there are two possible polarizations of the waves one has to multiply with an additional factor 2. The number of modes per unit wavelength is equal to

$$\frac{dN}{d\lambda}\times\frac{1}{L^3}=\frac{d}{d\lambda}\left[\frac{8\pi L^3}{3\lambda^3}\right]\times\frac{1}{L^3}=-\left[\frac{8\pi}{\lambda^4}\right]. \tag{B.5}$$

B.1.1 Classical approach

Following the principle of equipartition of energy, each standing wave mode will have an average enkergy kT with k the Boltzmann constant and T the temperature in Kelvin. The energy density is then:

$$\frac{du}{d\lambda} = -kT\frac{8\pi}{\lambda^4}. \tag{B.6}$$

In function of frequency $\nu = \frac{c}{\lambda}$:

$$\frac{du}{d\nu} = -\frac{c}{\lambda^2}\frac{du}{d\lambda} = \frac{8\pi kT\nu^2}{c^3}, \tag{B.7}$$

also known as the Rayleigh-Jeans law*. Problem: divergence

B.1.2 Quantum approach

The energy levels from a quantized harmonic oscillator are equal to

$$E_r = h\nu\left(r+\frac{1}{2}\right) = \frac{hc}{\lambda}\left(r+\frac{1}{2}\right) \quad \text{with} r = 0, 1, 2, ... \tag{B.8}$$

Implementing eq. B.4

$$E = \left(r+\frac{1}{2}\right)\frac{hc}{2L}\sqrt{n_1^2+n_2^2+n_3^2} \tag{B.9}$$

According to statistical physics the average energy is now not equal to kT but follows a probability distribution

$$p(\nu, r) = \frac{e^{\frac{-rh\nu}{kT}}}{\sum_{r=0}^{\infty} e^{\frac{-rh\nu}{kT}}}, \tag{B.10}$$

where we reference to the ground state of the oscillator: $E_r' = E_r - E_0$.

The average energy is now:

$$\begin{aligned}\langle E(\nu)\rangle &= \sum_{r=0}^{\infty} E(\nu, r)\cdot p(\nu, r) = \frac{\sum_{r=0}^{\infty} rh\nu\ e^{\frac{-rh\nu}{kT}}}{\sum_{r=0}^{\infty} e^{\frac{-rh\nu}{kT}}} \\ &= \frac{h\nu}{e^{h\nu/kT}-1}\end{aligned} \tag{B.11}$$

Substituting this for kT in eq. B.7 we find Planck's equation:

$$\frac{du}{d\nu} = \frac{8\pi h\nu^3}{c^3}\frac{h\nu}{e^{h\nu/kT}-1} \tag{B.12}$$

*This is often quoted per unit of staradian, which results in $\frac{2kT\nu^2}{c^3}$

C. Statistics

A word that is often mentioned in this work is “statistics”. It refers to the statistical error of a counting experiment, i.e. the Poissonian error. The Poisson distribution is a discrete probability of a certain number of $n$events occurring in a fixed time interval. The Poisson probability function is given by

$$P(n) = \frac{\lambda^n e^{-\lambda}}{n!}, \tag{C.1}$$

where λ is the expected number of events and also equal to the variance. An experiment that counted N events therefore has a statistical error of

$$\sigma = \sqrt{N} \tag{C.2}$$

In other words: higher statistics denotes a lower statistical error.

D. Distributions

D.1 Spherical random numbers

Most random number generators provide uniform distributions between the range $[0, 1]$. Assume we want to make a uniform distribution along a sphere with angles ϕ and θ and radius r, in spherical coordinates. Random numbers between $[0, \pi]$, $[0, 2\pi]$ and $[0, R]$ (the ranges of the coordinates) would not give a uniform distribution as illustrated in Fig. D.1 (left).

The differential surface area, dA, is equal to $dA(d\phi, d\theta) = r^2 \sin(\phi) d\phi d\theta$. If we want the distribution $f(v)$ to be constant for a uniform distribution, then $f(v) = \frac{1}{4\pi}$ since $\int\int_S f(v) dA = 1$ and $\int\int_S dA = 4\pi$. We want the distribution in function of the angles, so

$$f(v)dA = \frac{1}{4\pi} dA = f(r) f(\phi, \theta) d\phi d\theta. \tag{D.1}$$

Since we know the expression for dA, we find that

$$f(\phi, \theta) = \frac{1}{4\pi} \sin(\phi), \tag{D.2}$$

and separating the angles:

$$f(\theta) = \int_0^{\pi} f(\phi, \theta) d\phi = \frac{1}{2\pi}, \tag{D.3}$$

$$f(\phi) = \int_0^{2\pi} f(\phi, \theta) d\theta = \frac{\sin(\phi)}{2}, \tag{D.4}$$

where it is clear that $f(\phi)$ scales with $\sin(\phi)$; there are more points needed at the equator (this makes sense, as the surface at the equator is much larger!).

The question is now how one can get a sample to follow the distribution of $f(\phi)$. For this, we use the *inverse transform sampling* method where one makes use of the cumulative distribution function, $F(\phi)$, which increases monotonically

$$F(\phi) = \int_0^{\phi} f(\phi') d\phi' = \frac{1}{2} (1 - \cos(\phi)). \tag{D.5}$$

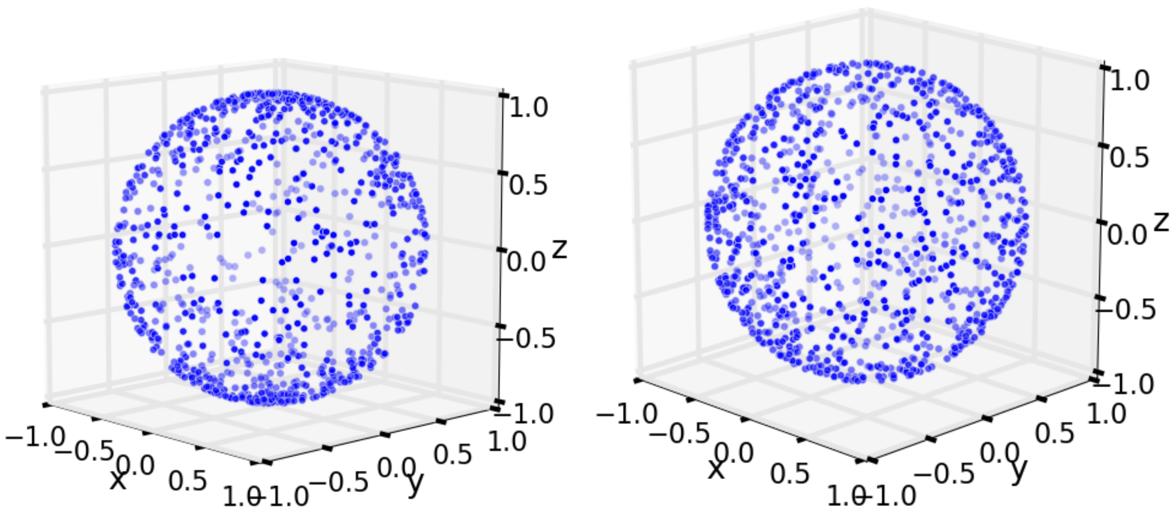

Figure D.1: *Left:* Illustration of a uniform sampling in angles ϕ and θ that doesn't give a uniform spherical distribution. *Right:* Illustration of a good spherical distribution.

The method shows that if u is a random variable drawn from a uniform distribution, we have to find the inverse function of F,

$$
\begin{aligned}
F(F^{-1}(u)) &= u && \text{(D.6)}\\
\frac{1}{2}\left(1-\cos(F^{-1}(u))\right) &= u && \text{(D.7)}\\
F^{-1}(u) &= \arccos(1-2u). && \text{(D.8)}
\end{aligned}
$$

In other words: if u is a random variable drawn from a uniform distribution, then $\phi = \arccos(1-2u)$ follows a distribution necessary for a uniform spherical distribution. Similarly, $\theta = \frac{1}{2\pi}u$.

D.2 Power law distributions

Analogous to what was written in the previous section, one can produce a power law distribution from random numbers using the inverse transform sampling method:

$$
\begin{aligned}
f(E) &= A \cdot E^{-\gamma} \quad \text{(powerlaw)}\\
F(E) &= \int_{E_{min}}^{E} A \cdot E^{-\gamma} dE = u \quad \text{(inverse sampling, u random number [0,1])}\\
&= A\left[\frac{E^{-\gamma+1}}{-\gamma+1}\right]_{E_{min}}^{E}\\
&= \frac{A}{-\gamma+1}\left(E^{-\gamma+1} - E_{min}^{-\gamma+1}\right)
\end{aligned}
\tag{D.9}
$$

Because we know that $F\left(F^{-1}(u)\right) = u$, we can find an expression for $F^{-1}(u)$:

$$
\begin{aligned}
u &= \frac{A}{-\gamma+1}\left(\left(F^{-1}(u)\right)^{-\gamma+1} - E_{min}^{-\gamma+1}\right)\\
&\Rightarrow\\
F^{-1}(u) &= \left(\left(\frac{-\gamma+1}{A}\cdot u\right) + E_{min}^{-\gamma+1}\right)^{1/(-\gamma+1)}
\end{aligned}
\quad .
\tag{D.10}
$$

To find A, we use the property of a CDF:

$$F(E_{max}) = 1 \Rightarrow A = \frac{-\gamma + 1}{E_{max}^{-\gamma+1} - E_{min}^{-\gamma+1}}, \tag{D.11}$$

leading to

$$F^{-1}(u) = \left((1-u) \cdot E_{min}^{-\gamma+1} + u \cdot E_{max}^{-\gamma+1}\right)^{1/(-\gamma+1)}, \tag{D.12}$$

which shows how one can draw a distribution in function of E following $f(E)$ with a uniform random number u.

For γ = -1, the computations are analogous and one can see that this will produce a uniform distribution in log space. This is shown in Fig. D.2.

$$\begin{aligned} E &= E_{min} \cdot 10^{u \cdot \log \frac{E_{max}}{E_{min}}} \\ &= 10^{u[\log E_{min}, \log E_{max}]} \end{aligned} \tag{D.13}$$

D.3 Angular distributions

As seen in Section D.1, the differential space angle $d\Omega$ is equal to

$$d\Omega = \sin(\theta) d\theta d\phi. \tag{D.14}$$

If one shows the distribution of ϕ and/or θ, then this is the same as showing partial integrations per bin. We find that

$$\Omega \propto \cos(\theta), \tag{D.15}$$

or in other words: the space angle is proportional to the azimuth and the cosine of the zenith. An example is shown in Fig. D.3.

D.4 Weighting

A method that is often used in simulations is *weighting*. The simulated and expected differential flux of particles is often not the same, mainly due to two reasons:

- The flux has no uniform power law behavior. As can bee seen in Fig. **??**, there can be multiple "kinks" and changes in a spectrum. Instead of simulating the flux according to one model, a general uniform flux is used and later reweighted to be able to fit to other models more easily.
- A steep power law indicates very few events at the highest energy bins. This means large CPU time would be necessary to simulate these events. As an example, let us assume two different fluxes

$$f_1 = A \cdot x^{-1}, \tag{D.16}$$

$$f_2 = B \cdot x^{-2}, \tag{D.17}$$

where $A = 10^3$ and $B = 10^4$, so the fluxes cross at a value of $x^{-1+2} = x = \frac{10^4}{10^3} = 10$. In the interval $x \in [10^3, 10^4]$, the number of events for f_1 is equal to 10^3, whereas for f_2 this is equal to 9.

Simulating with harder spectra* leads to more statistics in high-energy bins.

*Harder spectra equals to a lower gamma, since there will be more high-energy events.

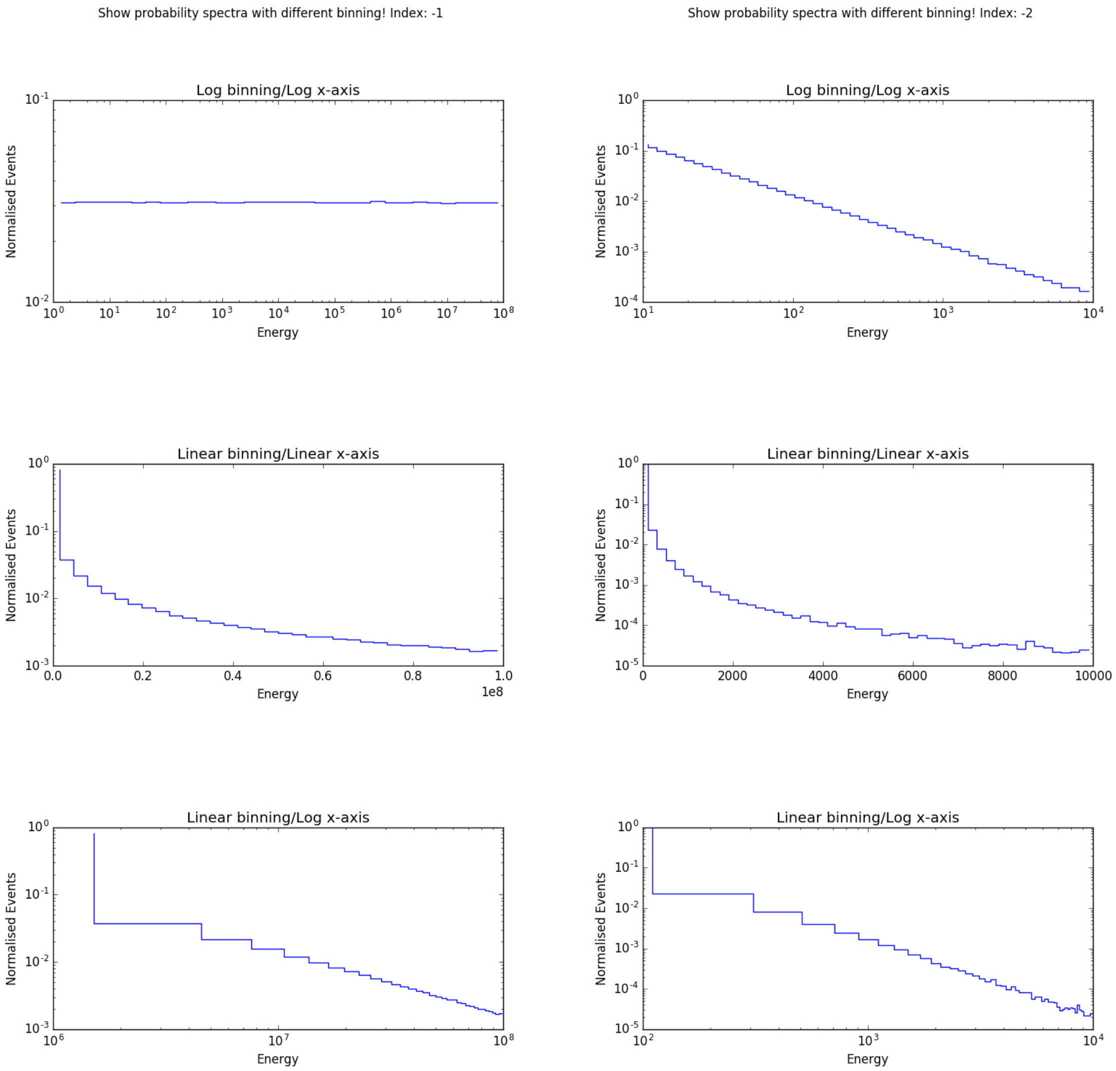

Figure D.2: *Left:* Histograms with different binnings showing the behavior of an energy spectrum with spectral index -1. *Right:* Histograms with different binnings showing the behavior of an energy spectrum with spectral index -2.

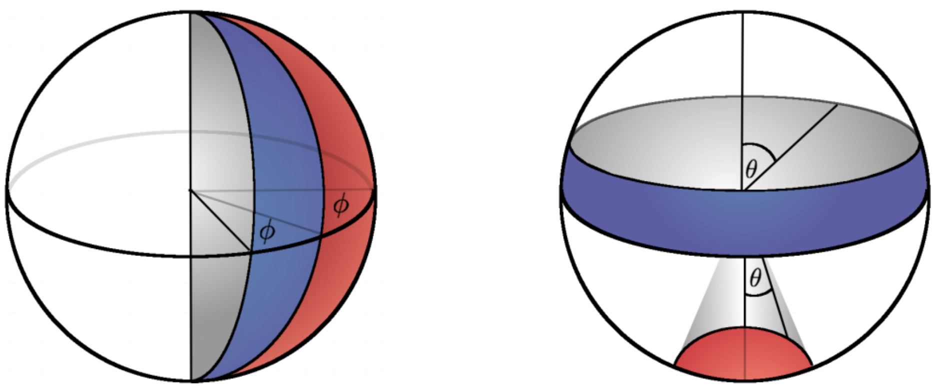

Figure D.3: Illustration of angle distributions in spherical coordinates. The blue and red surfaces are equal in size. The left figure clearly shows the surface to be proportional to the azimuth. The right figure shows how there is a non-trivial dependence on the zenith angle for equal partitions on the surface of a sphere.

The weights can be generally written down as

$$w = \frac{dN_{exp}}{dAd\Omega dEdt} \times \frac{dAd\Omega dE}{dN_{sim}}. \tag{D.18}$$

A disadvantage of using weights is that certain events with a high weight are rare but can dominate or obscure the sample in the tails of certain distributions.

E. AdaBoost: simple example

Consider a binary decision tree classification with 10 training examples. The illustrations below are 2D variable distributions.

We give each event an equal weight, making the weight distribution D_1 uniform. For this simple example, each of our classifiers will be an axis-parallel linear classifier (simple cut in one of the two variables).

Initial distribution

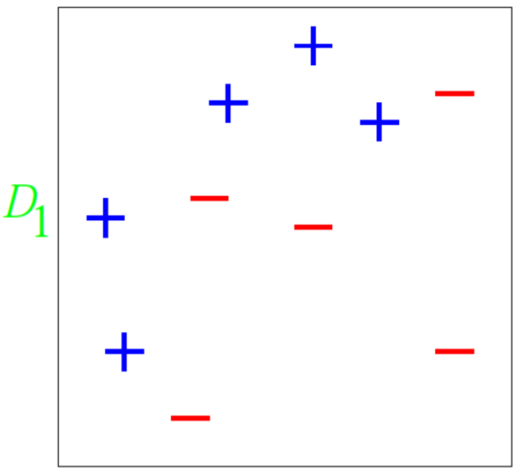

Round 1

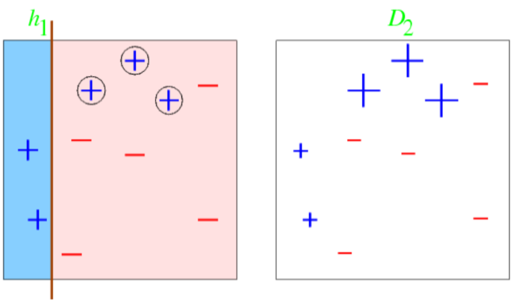

- Error rate of h_1: $\epsilon_1 = 0.3$; weight of h_1 (see Eq. **??**): $\alpha_1 = \frac{1}{2}\ln\left(\frac{1-\epsilon_1}{\epsilon_1}\right) = 0.42$

- An event that is misclassified gets a higher weight: weight multiplied with $\exp(\alpha_1)$
- An event that is correcly classified gets a lower weight: weight multiplied with $\exp(-\alpha_1)$

Round 2

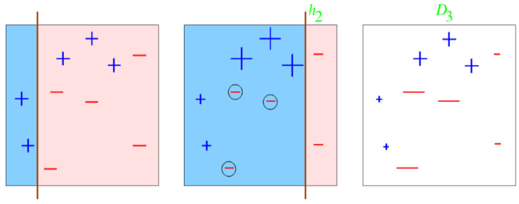

- Error rate of h_1: $\epsilon_1 = 0.21$; weight of h_2 (see Eq. **??**): $\alpha_2 = \frac{1}{2}\ln\left(\frac{1-\epsilon_2}{\epsilon_2}\right) = 0.65$
- An event that is misclassified gets a higher weight: weight multiplied with $\exp(\alpha_2)$
- An event that is correcly classified gets a lower weight: weight multiplied with $\exp(-\alpha_2)$

Round 3

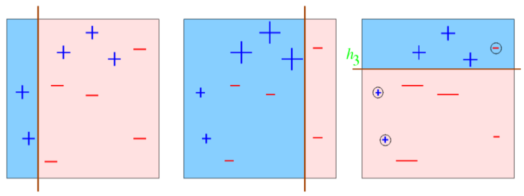

The error rate of h_1: $\epsilon_1 = 0.21$; weight of h_2 (see Eq. **??**): $\alpha_2 = \frac{1}{2}\ln\left(\frac{1-\epsilon_2}{\epsilon_2}\right) = 0.65$
Let us suppose to stop after this round, we now have a forest of 3 decision classifiers: h_1, h_2, h_3.

Final step

The final classifier is a weighted linear combination of all the classifiers:

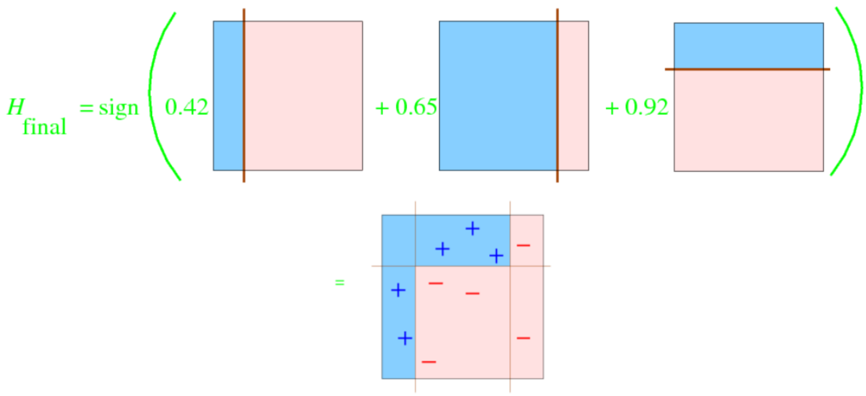

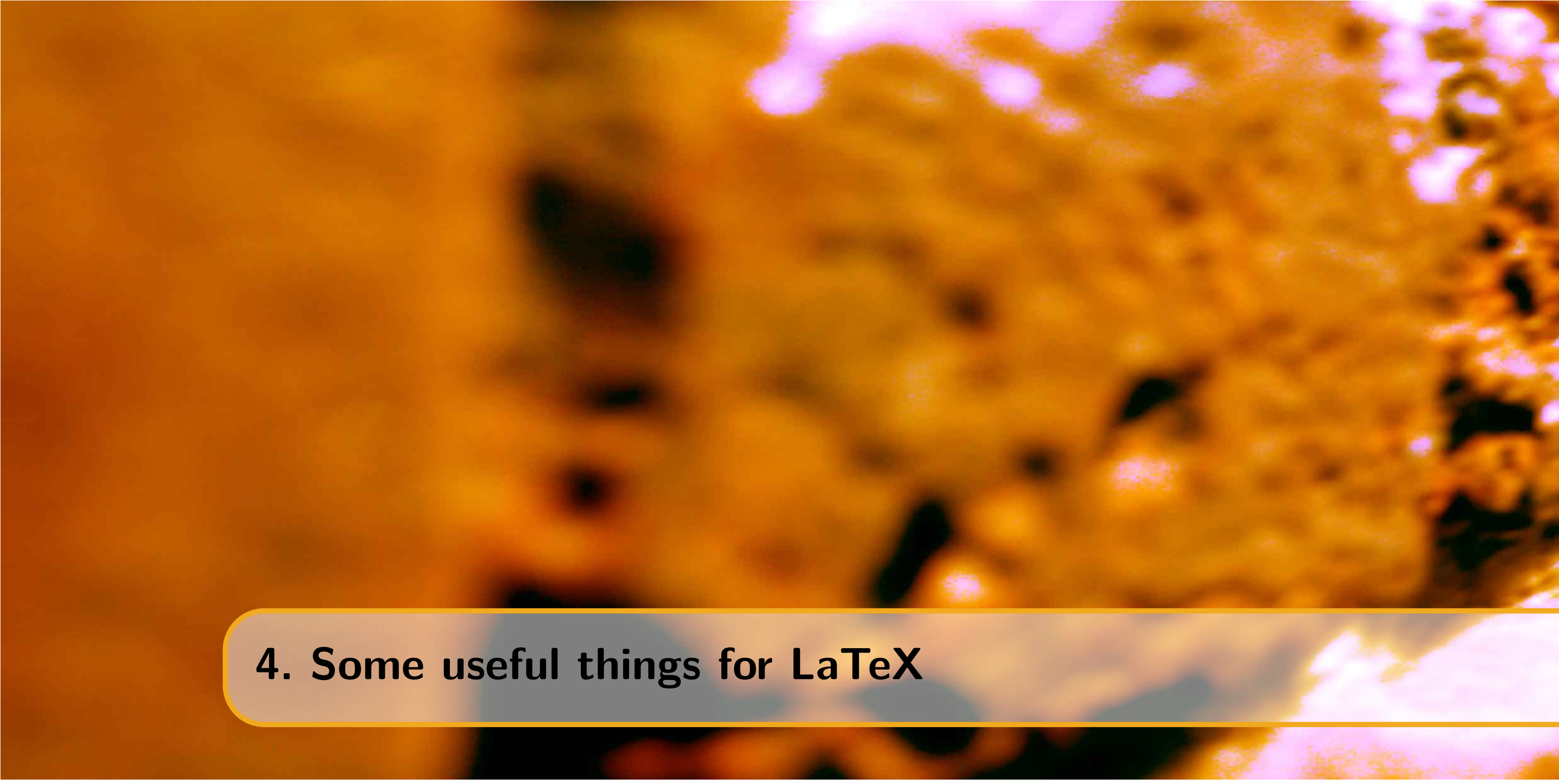

4. Some useful things for LaTeX

4.1 Definitions

This is an example of a definition. A definition could be mathematical or it could define a concept.

Definition 4.1.1 — Definition name. Given a vector space E, a norm on E is an application, denoted $||\cdot||$, E in $\mathbb{R}^+ = [0, +\infty[$ such that:

$$||\mathbf{x}|| = 0 \;\Rightarrow\; \mathbf{x} = \mathbf{0} \tag{4.1}$$

$$||\lambda\mathbf{x}|| = |\lambda| \cdot ||\mathbf{x}|| \tag{4.2}$$

$$||\mathbf{x} + \mathbf{y}|| \leq ||\mathbf{x}|| + ||\mathbf{y}|| \tag{4.3}$$

4.2 Remarks

This is an example of a remark.

R The concepts presented here are now in conventional employment in mathematics. Vector spaces are taken over the field $\mathbb{K} = \mathbb{R}$, however, established properties are easily extended to $\mathbb{K} = \mathbb{C}$.

4.3 Corollaries

This is an example of a corollary.

Corollary 4.3.1 — Corollary name. The concepts presented here are now in conventional employment in mathematics. Vector spaces are taken over the field $\mathbb{K} = \mathbb{R}$, however, established properties are easily extended to $\mathbb{K} = \mathbb{C}$.

4.4 Propositions

This is an example of propositions.

4.4.1 Several equations

Proposition 4.4.1 — Proposition name. It has the properties:

$$\left| ||\mathbf{x}|| - ||\mathbf{y}|| \right| \leq ||\mathbf{x} - \mathbf{y}|| \tag{4.4}$$

$$||\sum_{i=1}^{n} \mathbf{x}_i|| \leq \sum_{i=1}^{n} ||\mathbf{x}_i|| \quad \text{where } n \text{ is a finite integer} \tag{4.5}$$

4.4.2 Single Line

Proposition 4.4.2 Let $f, g \in L^2(G)$; if $\forall \varphi \in \mathcal{D}(G)$, $(f, \varphi)_0 = (g, \varphi)_0$ then $f = g$.

4.5 Examples

This is an example of examples.

4.5.1 Equation and Text

■ **Example 4.1** Let $G = \{x \in \mathbb{R}^2 : |x| < 3\}$ and denoted by: $x^0 = (1, 1)$; consider the function:

$$f(x) = \begin{cases} \mathrm{e}^{|x|} & \text{si } |x - x^0| \leq 1/2 \\ 0 & \text{si } |x - x^0| > 1/2 \end{cases} \tag{4.6}$$

The function f has bounded support, we can take $A = \{x \in \mathbb{R}^2 : |x - x^0| \leq 1/2 + \epsilon\}$ for all $\epsilon \in \,]0\,; 5/2 - \sqrt{2}[$. ■

4.5.2 Paragraph of Text

■ **Example 4.2 — Example name.** Nam dui ligula, fringilla a, euismod sodales, sollicitudin vel, wisi. Morbi auctor lorem non justo. Nam lacus libero, pretium at, lobortis vitae, ultricies et, tellus. Donec aliquet, tortor sed accumsan bibendum, erat ligula aliquet magna, vitae ornare odio metus a mi. Morbi ac orci et nisl hendrerit mollis. Suspendisse ut massa. Cras nec ante. Pellentesque a nulla. Cum sociis natoque penatibus et magnis dis parturient montes, nascetur ridiculus mus. Aliquam tincidunt urna. Nulla ullamcorper vestibulum turpis. Pellentesque cursus luctus mauris.

■

4.6 Exercises

This is an example of an exercise.

Exercise 4.1 This is a good place to ask a question to test learning progress or further cement ideas into students' minds. ■

4.7 Problems

Problem 4.1 What is the average airspeed velocity of an unladen swallow?

4.8 Vocabulary

Define a word to improve a students' vocabulary.

Vocabulary 4.1 — Word. Definition of word.

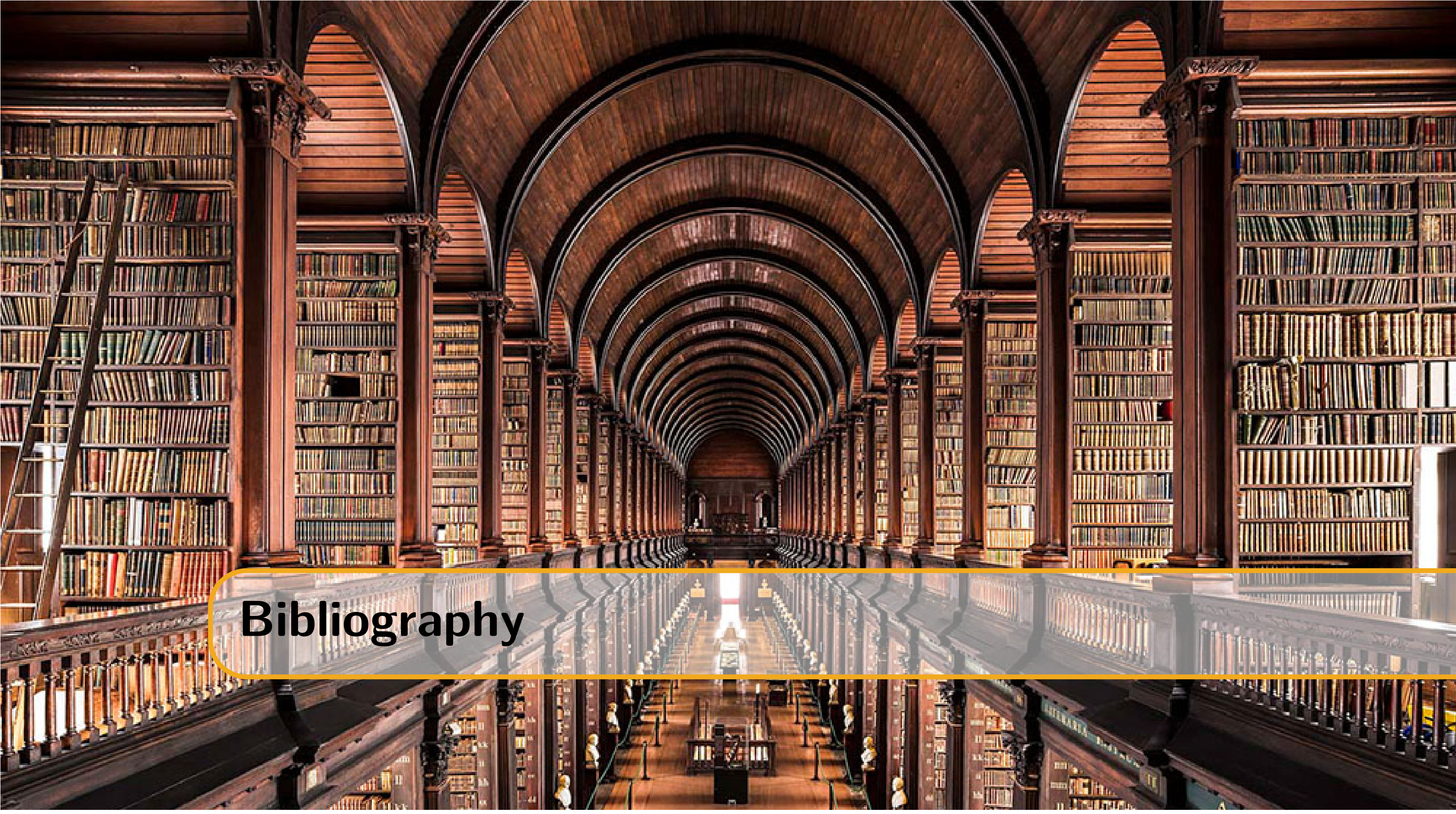

Bibliography

[1] B. Povh et al. *Particles and nuclei: An Introduction to the physical concepts*. 1995. DOI: 10.1007/3-540-36684-9.

[2] Michael E. Peskin and Daniel V. Schroeder. *An Introduction to quantum field theory*. Reading, USA: Addison-Wesley, 1995. ISBN: 9780201503975, 0201503972. URL: http://www.slac.stanford.edu/~mpeskin/QFT.html.

[3] M. Tanabashi et al. "Review of Particle Physics". In: *Phys. Rev. D* 98 (2018), page 030001.

[4] Alessandro Bettini. *Introduction to elementary particle physics*. 2008. ISBN: 9780521880213. URL: http://www.cambridge.org/catalogue/catalogue.asp?isbn=9780521880213.

[5] CERN. URL: https://home.cern/about/physics/standard-model.

[6] Arthur B. McDonald. "Nobel Lecture: The Sudbury Neutrino Observatory: Observation of flavor change for solar neutrinos". In: *Rev. Mod. Phys.* 88 (3 July 2016), page 030502. DOI: 10.1103/RevModPhys.88.030502. URL: https://link.aps.org/doi/10.1103/RevModPhys.88.030502.

[7] CMS. URL: http://cms.web.cern.ch/news/jets-cms-and-determination-their-energy-scale.

[8] A. Kircher. *Athanasii Kircherii... Magnes, sive De arte magnetica opus tripartitum...* sumptibus H. Scheus, 1641. URL: https://books.google.be/books?id=1aZ3FcTAYdUC.

[9] G. Farmelo. *The Strangest Man: The Hidden Life of Paul Dirac, Mystic of the Atom*. Basic Books, 2009. ISBN: 9780465019922. URL: https://books.google.be/books?id=qsodmIGD0fMC.

[10] F. Mandl and G. Shaw. *Quantum Field Theory*. Wiley, 2013. ISBN: 9781118716656. URL: https://books.google.be/books?id=jTBzQfctvHAC.

[11] Flip Tanedo. URL: https://www.quantumdiaries.org/2012/02/14/why-do-we-expect-a-higgs-boson-part-ii-unitarization-of-vector-boson-scattering/.

[12] S. L. Glashow, J. Iliopoulos, and L. Maiani. "Weak Interactions with Lepton-Hadron Symmetry". In: *Phys. Rev.* D2 (1970), pages 1285–1292. DOI: 10.1103/PhysRevD.2.1285.

[13] J. H. Christenson et al. "Evidence for the 2π Decay of the K20 Meson". In: *Physical Review Letters* 13 (July 1964), pages 138–140. DOI: 10.1103/PhysRevLett.13.138.

[14] Ziro Maki, Masami Nakagawa, and Shoichi Sakata. "Remarks on the Unified Model of Elementary Particles". In: *Progress of Theoretical Physics* 28.5 (1962), pages 870–880. DOI: 10.1143/PTP.28.870. eprint: /oup/backfile/content_public/journal/ptp/28/5/10.1143/ptp.28.870/2/28-5-870.pdf. URL: http://dx.doi.org/10.1143/PTP.28.870.

[15] Unknown. *Young interference*. https://www.shmoop.com/optics/young-double-slit.html. [Online; accessed August 2018]. 2018.

[16] Antoine Weis and Robert Wynands. "Three Demonstration Experiments on the Wave and Particle Nature of Light". In: 1 (June 2003).

[17] C. Davisson and L. H. Germer. "Diffraction of Electrons by a Crystal of Nickel". In: *Phys. Rev.* 30 (1927), pages 705–740. DOI: 10.1103/PhysRev.30.705.

[18] G P. Thomson and Reid AA. "Diffraction of Cathode Rays by a Thin Film". In: 119 (Jan. 1927), pages 890–890.

[19] Claus Jönsson. "Elektroneninterferenzen an mehreren künstlich hergestellten Feinspalten". In: *Zeitschrift für Physik* 161.4 (Aug. 1961), pages 454–474. ISSN: 0044-3328. DOI: 10.1007/BF01342460. URL: https://doi.org/10.1007/BF01342460.

[20] P G Merli, G F Missiroli, and G Pozzi. "Electron interferometry with the Elmiskop 101 electron microscope". In: *Journal of Physics E: Scientific Instruments* 7.9 (1974), page 729. URL: http://stacks.iop.org/0022-3735/7/i=9/a=016.

[21] C. D. Anderson. "The Positive Electron". In: *Phys. Rev.* 43 (1933), pages 491–494. DOI: 10.1103/PhysRev.43.491.

[22] Paul A. M. Dirac. "The quantum theory of the electron". In: *Proc. Roy. Soc. Lond.* A117 (1928), pages 610–624. DOI: 10.1098/rspa.1928.0023.

[23] C. M. G. Lattes et al. "PROCESSES INVOLVING CHARGED MESONS". In: *Nature* 159 (1947). [,42(1947)], pages 694–697. DOI: 10.1038/159694a0.

[24] S. H. Neddermeyer and C. D. Anderson. "Note on the Nature of Cosmic Ray Particles". In: *Phys. Rev.* 51 (1937), pages 884–886. DOI: 10.1103/PhysRev.51.884.

[25] S. W. Herb et al. "Observation of a Dimuon Resonance at 9.5-GeV in 400-GeV Proton-Nucleus Collisions". In: *Phys. Rev. Lett.* 39 (1977), pages 252–255. DOI: 10.1103/PhysRevLett.39.252.

[26] F. Abe et al. "Observation of top quark production in $\bar{p}p$ collisions". In: *Phys. Rev. Lett.* 74 (1995), pages 2626–2631. DOI: 10.1103/PhysRevLett.74.2626. arXiv: hep-ex/9503002 [hep-ex].

[27] D. P. Barber et al. "Discovery of Three Jet Events and a Test of Quantum Chromodynamics at PETRA Energies". In: *Phys. Rev. Lett.* 43 (1979), page 830. DOI: 10.1103/PhysRevLett.43.830.

[28] S. Schael et al. "Precision electroweak measurements on the Z resonance". In: *Phys. Rept.* 427 (2006), pages 257–454. DOI: 10.1016/j.physrep.2005.12.006. arXiv: hep-ex/0509008 [hep-ex].

[29] Sabine Riemann. "Precision electroweak physics at high energies". In: *Rept. Prog. Phys.* 73 (2010), page 126201. DOI: 10.1088/0034-4885/73/12/126201.

[30] Kenji Abe et al. "A High precision measurement of the left-right Z boson cross-section asymmetry". In: *Phys. Rev. Lett.* 84 (2000), pages 5945–5949. DOI: 10.1103/PhysRevLett.84.5945. arXiv: hep-ex/0004026 [hep-ex].

[31] Koya Abe et al. "First direct measurement of the parity violating coupling of the Z0 to the s quark". In: *Phys. Rev. Lett.* 85 (2000), pages 5059–5063. DOI: 10.1103/PhysRevLett.85.5059. arXiv: hep-ex/0006019 [hep-ex].

[32] Koya Abe et al. "An Improved direct measurement of leptonic coupling asymmetries with polarized Z bosons". In: *Phys. Rev. Lett.* 86 (2001), pages 1162–1166. DOI: 10.1103/PhysRevLett.86.1162. arXiv: hep-ex/0010015 [hep-ex].

[33] K. Abe et al. "First measurement of the left-right charge asymmetry in hadronic Z boson decays and a new determination of sin**2 theta(W)(eff)". In: *Phys. Rev. Lett.* 78 (1997), pages 17–21. DOI: 10.1103/PhysRevLett.78.17. arXiv: hep-ex/9609019 [hep-ex].

[34] Timo Antero Aaltonen et al. "Combination of CDF and D0 W-Boson Mass Measurements". In: *Phys. Rev.* D88.5 (2013), page 052018. DOI: 10.1103/PhysRevD.88.052018. arXiv: 1307.7627 [hep-ex].

[35] "Combination of CDF and D0 Results on the Width of the W boson". In: (2010). arXiv: 1003.2826 [hep-ex].

[36] Morad Aaboud et al. "Measurement of the W-boson mass in pp collisions at $\sqrt{s} = 7$ TeV with the ATLAS detector". In: *Eur. Phys. J.* C78.2 (2018), page 110. DOI: 10.1140/epjc/s10052-017-5475-4. arXiv: 1701.07240 [hep-ex].

[37] ATLAS. URL: cds.cern.ch/record/2285809/files/ATLAS-CONF-2017-071.pdf.

[38] CMS. URL: cds.cern.ch/record/2235162/files/TOP-15-012-pas.pdf.

[39] CMS. URL: cds.cern.ch/record/2284594/files/TOP-17-007-pas.pdf.

[40] PDG. URL: http://pdg.lbl.gov/2018/reviews/rpp2018-rev-standard-model.pdf.

[41] P. A. R. Ade et al. "Planck 2015 results. XIII. Cosmological parameters". In: *Astron. Astrophys.* 594 (2016), A13. DOI: 10.1051/0004-6361/201525830. arXiv: 1502.01589 [astro-ph.CO].

[42] Edvige Corbelli and Paolo Salucci. "The Extended Rotation Curve and the Dark Matter Halo of M33". In: *Mon. Not. Roy. Astron. Soc.* 311 (2000), pages 441–447. DOI: 10.1046/j.1365-8711.2000.03075.x. arXiv: astro-ph/9909252 [astro-ph].

[43] S. M. Faber and R. E. Jackson. "Velocity dispersions and mass to light ratios for elliptical galaxies". In: *Astrophys. J.* 204 (1976), page 668. DOI: 10.1086/154215.

[44] Steven W. Allen, August E. Evrard, and Adam B. Mantz. "Cosmological Parameters from Observations of Galaxy Clusters". In: *Ann. Rev. Astron. Astrophys.* 49 (2011), pages 409–470. DOI: 10.1146/annurev-astro-081710-102514. arXiv: 1103.4829 [astro-ph.CO].

[45] Priyamvada Natarajan et al. "Mapping substructure in the HST Frontier Fields cluster lenses and in cosmological simulations". In: *Mon. Not. Roy. Astron. Soc.* 468.2 (2017), pages 1962–1980. DOI: 10.1093/mnras/stw3385. arXiv: 1702.04348 [astro-ph.GA].

[46] Edwin Hubble. "A relation between distance and radial velocity among extra-galactic nebulae". In: *Proc. Nat. Acad. Sci.* 15 (1929), pages 168–173. DOI: 10.1073/pnas.15.3.168.

[47] John F. Donoghue. "The effective field theory treatment of quantum gravity". In: *AIP Conf. Proc.* 1483 (2012), pages 73–94. DOI: 10.1063/1.4756964. arXiv: 1209.3511 [gr-qc].

[48] J. L. Holzbauer. "The Muon g-2 Experiment Overview and Status". In: *PoS* NuFact2017 (2018), page 116. DOI: 10.22323/1.295.0116. arXiv: 1712.05980 [hep-ex].

[49] Alexandre Deur, Stanley J. Brodsky, and Guy F. de Teramond. "The QCD Running Coupling". In: *Prog. Part. Nucl. Phys.* 90 (2016), pages 1–74. DOI: 10.1016/j.ppnp.2016.04.003. arXiv: 1604.08082 [hep-ph].

[50] nobel2004. URL: https://www.nobelprize.org/prizes/physics/2004/popular-information/.

[51] Xiao-Gang He, Girish C. Joshi, and B. H. McKellar. "The Quantization of the Electric Charge in Gauge Theories". In: *Europhys. Lett.* 10 (1989), page 709. DOI: 10.1209/0295-5075/10/8/002.

[52] Hong-Wei Yu. "SU(8) GUT MODELS WITH STABLE PROTON, N ANTI-N OSCILLATIONS, FRACTIONAL CHARGES AND LOW MASS MONOPOLES". In: *Phys. Lett.* 142B (1984), pages 42–46. DOI: 10.1016/0370-2693(84)91132-8.

[53] Stephen M. Barr, D. B. Reiss, and A. Zee. "Fractional Charges, Monopoles and Peculiar Photons". In: *Phys. Rev. Lett.* 50 (1983), page 317. DOI: 10.1103/PhysRevLett.50.317.

[54] P. H. Frampton and T. W. Kephart. "Fractionally Charged Particles as Evidence for Supersymmetry". In: *Phys. Rev. Lett.* 49 (1982), page 1310. DOI: 10.1103/PhysRevLett.49.1310.

[55] Katsuji Yamamoto. "Fractionally Charged Leptons in the SO(14) GUT". In: *Phys. Lett.* 120B (1983), pages 157–160. DOI: 10.1016/0370-2693(83)90643-3.

[56] Fang-xiao Dong et al. "Fractional Charges, Monopoles and Peculiar Photons in SO(18) GUT Models". In: *Phys. Lett.* 129B (1983), pages 405–410. DOI: 10.1016/0370-2693(83)90129-6.

[57] Xiang-Dong Jiang and Xian-Jian Zhou. "SO(10) X SO(8) MODEL WITH FRACTIONAL CHARGES, MONOPOLES AND PECULIAR PHOTONS. (IN CHINESE)". In: *HEPNP* 9 (1985), pages 421–429.

[58] Borut Bajc et al. "Threshold corrections to dimension-six proton decay operators in non-minimal SUSY SU (5) GUTs". In: *Nucl. Phys.* B910 (2016), pages 1–22. DOI: 10.1016/j.nuclphysb.2016.06.017. arXiv: 1603.03568 [hep-ph].

[59] H. Nishino et al. "Search for Proton Decay via p —> e+ pi0 and p —> mu+ pi0 in a Large Water Cherenkov Detector". In: *Phys. Rev. Lett.* 102 (2009), page 141801. DOI: 10.1103/PhysRevLett.102.141801. arXiv: 0903.0676 [hep-ex].

[60] Xiao-Gang Wen and Edward Witten. "Electric and Magnetic Charges in Superstring Models". In: *Nucl. Phys.* B261 (1985), pages 651–677. DOI: 10.1016/0550-3213(85)90592-9.

[61] Ignatios Antoniadis and K. Benakli. "Fractionally charged particles and supersymmetry breaking in 4-D strings". In: *Phys. Lett.* B295 (1992). [Erratum: Phys. Lett.B407,449(1997)], pages 219–224. DOI: 10.1016/S0370-2693(97)00755-7,10.1016/0370-2693(92)91557-P. arXiv: hep-th/9209020 [hep-th].

[62] Gregory G. Athanasiu et al. "Remarks on Wilson Lines, Modular Invariance and Possible String Relics in Calabi-yau Compactifications". In: *Phys. Lett.* B214 (1988), pages 55–62. DOI: 10.1016/0370-2693(88)90451-0.

[63] Bob Holdom. "Two U(1)'s and Epsilon Charge Shifts". In: *Phys. Lett.* 166B (1986), pages 196–198. DOI: 10.1016/0370-2693(86)91377-8.

[64] Eder Izaguirre and Itay Yavin. "New window to millicharged particles at the LHC". In: *Phys. Rev.* D92.3 (2015), page 035014. DOI: 10.1103/PhysRevD.92.035014. arXiv: 1506.04760 [hep-ph].

[65] David E. Brahm and Lawrence J. Hall. "U(1)-prime DARK MATTER". In: *Phys. Rev.* D41 (1990), page 1067. DOI: 10.1103/PhysRevD.41.1067.

[66] C. Boehm and Pierre Fayet. "Scalar dark matter candidates". In: *Nucl. Phys.* B683 (2004), pages 219–263. DOI: 10.1016/j.nuclphysb.2004.01.015. arXiv: hep-ph/0305261 [hep-ph].

[67] Maxim Pospelov, Adam Ritz, and Mikhail B. Voloshin. "Secluded WIMP Dark Matter". In: *Phys. Lett.* B662 (2008), pages 53–61. DOI: 10.1016/j.physletb.2008.02.052. arXiv: 0711.4866 [hep-ph].

[68] James D. Bjorken et al. "New Fixed-Target Experiments to Search for Dark Gauge Forces". In: *Phys. Rev.* D80 (2009), page 075018. DOI: 10.1103/PhysRevD.80.075018. arXiv: 0906.0580 [hep-ph].

[69] Gabriel Magill et al. "Millicharged particles in neutrino experiments". In: (2018). arXiv: 1806.03310 [hep-ph].

[70] R. Acciarri et al. "Long-Baseline Neutrino Facility (LBNF) and Deep Underground Neutrino Experiment (DUNE)". In: (2015). arXiv: 1512.06148 [physics.ins-det].

[71] M. Anelli et al. “A facility to Search for Hidden Particles (SHiP) at the CERN SPS”. In: (2015). arXiv: `1504.04956 [physics.ins-det]`.

[72] Marco Battaglieri et al. “US Cosmic Visions: New Ideas in Dark Matter 2017: Community Report”. In: (2017). arXiv: `1707.04591 [hep-ph]`.

[73] S. I. Alvis et al. “First Limit on the Direct Detection of Lightly Ionizing Particles for Electric Charge as Low as e/1000 with the Majorana Demonstrator”. In: *Phys. Rev. Lett.* 120.21 (2018), page 211804. DOI: `10.1103/PhysRevLett.120.211804`. arXiv: `1801.10145 [hep-ex]`.

[74] L. Lyons. “Quark Search Experiments at Accelerators and in Cosmic Rays”. In: *Phys. Rept.* 129 (1985), page 225. DOI: `10.1016/0370-1573(85)90011-0`.

[75] J. J. Aubert et al. “A Search for Free Quarks in Deep Inelastic Muon Scattering”. In: *Phys. Lett.* 133B (1983), page 461. DOI: `10.1016/0370-2693(83)90828-6`.

[76] A. E. Bondar et al. “SEARCH FOR LIGHT PARTICLES WITH CHARGE 2/3 IN e+ e- ANNIHILATION”. In: *JETP Lett.* 40 (1984). [Pisma Zh. Eksp. Teor. Fiz.40,440(1984)], pages 1265–1268.

[77] H. Aihara et al. “Search for $q = 2/3e$ and $q = 1/3e$ particles produced in e^+e^- annihilations”. In: *Phys. Rev. Lett.* 52 (1984), page 2332. DOI: `10.1103/PhysRevLett.52.2332`.

[78] G. Abbiendi et al. “Search for stable and longlived massive charged particles in e+ e- collisions at s**(1/2) = 130-GeV to 209-GeV”. In: *Phys. Lett.* B572 (2003), pages 8–20. DOI: `10.1016/S0370-2693(03)00639-7`. arXiv: `hep-ex/0305031 [hep-ex]`.

[79] P. Abreu et al. “Search for stable heavy charged particles in e+ e- collisions at s**(1/2) = 130-GeV to 136-GeV, 161-GeV and 172-GeV”. In: *Phys. Lett.* B396 (1997), pages 315–326. DOI: `10.1016/S0370-2693(97)00152-4`.

[80] R. Akers et al. “Search for heavy charged particles and for particles with anomalous charge in e^+e^- collisions at LEP”. In: *Z. Phys.* C67 (1995), pages 203–212. DOI: `10.1007/BF01571281`.

[81] D. Buskulic et al. “Search for particles with unexpected mass and charge in Z decays”. In: *Phys. Lett.* B303 (1993), pages 198–208. DOI: `10.1016/0370-2693(93)90066-Q`.

[82] M. Banner et al. “A New Search for Relativistic Particles With Fractional Electric Charge at the CERN $p\bar{p}$ Collider”. In: *Phys. Lett.* 156B (1985), pages 129–133. DOI: `10.1016/0370-2693(85)91368-1`.

[83] F. Abe et al. “Limits on the production of massive stable charged particles”. In: *Phys. Rev.* D46 (1992), R1889–R1894. DOI: `10.1103/PhysRevD.46.R1889`.

[84] D. Acosta et al. “Search for long-lived charged massive particles in $\bar{p}p$ collisions at $\sqrt{s} = 1.8$ TeV”. In: *Phys. Rev. Lett.* 90 (2003), page 131801. DOI: `10.1103/PhysRevLett.90.131801`. arXiv: `hep-ex/0211064 [hep-ex]`.

[85] Serguei Chatrchyan et al. “Search for fractionally charged particles in pp collisions at $\sqrt{s} = 7$ TeV”. In: *Phys. Rev.* D87.9 (2013), page 092008. DOI: `10.1103/PhysRevD.87.092008`. arXiv: `1210.2311 [hep-ex]`.

[86] M. Mori et al. “Search for fractionally charged particles in Kamiokande-II”. In: *Phys. Rev.* D43 (1991), pages 2843–2846. DOI: `10.1103/PhysRevD.43.2843`.

[87] M. Ambrosio et al. “Final search for lightly ionizing particles with the MACRO detector”. In: (2004). arXiv: `hep-ex/0402006 [hep-ex]`.

[88] Thomas K. Gaisser, Ralph Engel, and Elisa Resconi. *Cosmic Rays and Particle Physics*. Cambridge University Press, 2016. ISBN: 9780521016469, 9781316598917. URL: `http://www.cambridge.org/de/academic/subjects/physics/cosmology-relativity-and-gravitation/cosmic-rays-and-particle-physics-2nd-edition?format=HB`.

[89] The Nobel Prize. URL: https://www.nobelprize.org/prizes/physics/1936/ceremony-speech/.

[90] R. A. Millikan and G. H. Cameron. "The Origin of the Cosmic Rays". In: *Phys. Rev.* 32 (4 Oct. 1928), pages 533–557. DOI: 10.1103/PhysRev.32.533. URL: https://link.aps.org/doi/10.1103/PhysRev.32.533.

[91] J. Clay. *Penetrating radiation.* Volume 30. 1927, pages 1115–1127.

[92] M.H. Israel et al. "Isotopic Composition of Cosmic Rays: Results from the Cosmic Ray Isotope Spectrometer on the ACE Spacecraft". In: *Nuclear Physics A* 758 (2005). Nuclei in the Cosmos VIII, pages 201–208. ISSN: 0375-9474. DOI: https://doi.org/10.1016/j.nuclphysa.2005.05.038. URL: http://www.sciencedirect.com/science/article/pii/S037594740500686X.

[93] Pasquale Blasi. "The Origin of Galactic Cosmic Rays". In: *Astron. Astrophys. Rev.* 21 (2013), page 70. DOI: 10.1007/s00159-013-0070-7. arXiv: 1311.7346 [astro-ph.HE].

[94] Thomas K. Gaisser, Todor Stanev, and Serap Tilav. "Cosmic Ray Energy Spectrum from Measurements of Air Showers". In: *Front. Phys.(Beijing)* 8 (2013), pages 748–758. DOI: 10.1007/s11467-013-0319-7. arXiv: 1303.3565 [astro-ph.HE] (cited on pages 10, 12).

[95] M A Malkov and L O'C Drury. "Nonlinear theory of diffusive acceleration of particles by shock waves". In: *Reports on Progress in Physics* 64.4 (2001), page 429. URL: http://stacks.iop.org/0034-4885/64/i=4/a=201.

[96] "Detection of the Small Magellanic Cloud in gamma-rays with Fermi/LAT". In: *Astron. Astrophys.* 523 (2010), A46. DOI: 10.1051/0004-6361/201014855. arXiv: 1008.2127 [astro-ph.HE].

[97] W. D. Apel et al. "Kneelike structure in the spectrum of the heavy component of cosmic rays observed with KASCADE-Grande". In: *Phys. Rev. Lett.* 107 (2011), page 171104. DOI: 10.1103/PhysRevLett.107.171104. arXiv: 1107.5885 [astro-ph.HE].

[98] A. P. Garyaka et al. "All-particle primary energy spectrum in the 3-200 PeV energy range". In: *J. Phys.* G35 (2008), page 115201. DOI: 10.1088/0954-3899/35/11/115201. arXiv: 0808.1421 [astro-ph].

[99] Kenneth Greisen. "End to the cosmic ray spectrum?" In: *Phys. Rev. Lett.* 16 (1966), pages 748–750. DOI: 10.1103/PhysRevLett.16.748.

[100] G. T. Zatsepin and V. A. Kuzmin. "Upper limit of the spectrum of cosmic rays". In: *JETP Lett.* 4 (1966). [Pisma Zh. Eksp. Teor. Fiz.4,114(1966)], pages 78–80.

[101] J. Bellido et al. "Proceedings of Science". In: *ICRC* 301 (506 2017).

[102] Alexander Aab et al. "Observation of a Large-scale Anisotropy in the Arrival Directions of Cosmic Rays above 8×10^{18} eV". In: *Science* 357.6537 (2017), pages 1266–1270. DOI: 10.1126/science.aan4338. arXiv: 1709.07321 [astro-ph.HE].

[103] E. Waxman. "IceCube's Neutrinos: The beginning of extra-Galactic neutrino astrophysics?" In: *Proceedings, 9th Rencontres du Vietnam: Windows on the Universe: Quy Nhon, Vietnam, August 11-17, 2013.* 2013, pages 161–168. arXiv: 1312.0558 [astro-ph.HE].

[104] A. M. Hillas. "The Origin of Ultrahigh-Energy Cosmic Rays". In: *Ann. Rev. Astron. Astrophys.* 22 (1984), pages 425–444. DOI: 10.1146/annurev.aa.22.090184.002233.

[105] Pablo M. Bauleo and Julio Rodriguez Martino. "The dawn of the particle astronomy era in ultra-high-energy cosmic rays". In: *Nature* 458N7240 (2009), pages 847–851. DOI: 10.1038/nature07948.

[106] P. O. Lagage and C. J. Cesarsky. "The maximum energy of cosmic rays accelerated by supernova shocks". In: *Astron. Astrophys.* 125 (1983), pages 249–257.

[107] T. Stanev. *High Energy Cosmic Rays*. Springer Praxis Books. Springer Berlin Heidelberg, 2010. ISBN: 9783540851486. URL: https://books.google.be/books?id=1y9YEYHAfBMC.

[108] C. Megan Urry and Paolo Padovani. "Unified schemes for radio-loud active galactic nuclei". In: *Publ. Astron. Soc. Pac.* 107 (1995), page 803. DOI: 10.1086/133630. arXiv: astro-ph/9506063 [astro-ph].

[109] Robert Antonucci. "Unified models for active galactic nuclei and quasars". In: *Ann. Rev. Astron. Astrophys.* 31 (1993), pages 473–521. DOI: 10.1146/annurev.aa.31.090193.002353.

[110] Demosthenes Kazanas et al. "Toward a Unified AGN Structure". In: (2012). arXiv: 1206.5022 [astro-ph.HE].

[111] J. Abraham et al. "Correlation of the highest-energy cosmic rays with the positions of nearby active galactic nuclei". In: *Astropart. Phys.* 29 (2008). [Erratum: Astropart. Phys.30,45(2008)], pages 188–204. DOI: 10.1016/j.astropartphys.2008.06.004,10.1016/j.astropartphys.2008.01.002. arXiv: 0712.2843 [astro-ph].

[112] M. G. Aartsen et al. "Multimessenger observations of a flaring blazar coincident with high-energy neutrino IceCube-170922A". In: *Science* 361.6398 (2018), eaat1378. DOI: 10.1126/science.aat1378. arXiv: 1807.08816 [astro-ph.HE].

[113] Ray W. Klebesadel, Ian B. Strong, and Roy A. Olson. "Observations of Gamma-Ray Bursts of Cosmic Origin". In: *Astrophys. J.* 182 (1973), pages L85–L88. DOI: 10.1086/181225.

[114] C. A. Meegan et al. "Spatial distribution of gamma-ray bursts observed by BATSE". In: *Nature* 355 (1992), pages 143–145. DOI: 10.1038/355143a0.

[115] Tsvi Piran. "The physics of gamma-ray bursts". In: *Rev. Mod. Phys.* 76 (2004), pages 1143–1210. DOI: 10.1103/RevModPhys.76.1143. arXiv: astro-ph/0405503 [astro-ph].

[116] B. P. Abbott et al. "GW170817: Observation of Gravitational Waves from a Binary Neutron Star Inspiral". In: *Phys. Rev. Lett.* 119.16 (2017), page 161101. DOI: 10.1103/PhysRevLett.119.161101. arXiv: 1710.05832 [gr-qc].

[117] B. P. Abbott et al. "GW170814: A Three-Detector Observation of Gravitational Waves from a Binary Black Hole Coalescence". In: *Phys. Rev. Lett.* 119.14 (2017), page 141101. DOI: 10.1103/PhysRevLett.119.141101. arXiv: 1709.09660 [gr-qc].

[118] B.. P.. Abbott et al. "GW170608: Observation of a 19-solar-mass Binary Black Hole Coalescence". In: *Astrophys. J.* 851.2 (2017), page L35. DOI: 10.3847/2041-8213/aa9f0c. arXiv: 1711.05578 [astro-ph.HE].

[119] Benjamin P. Abbott et al. "GW170104: Observation of a 50-Solar-Mass Binary Black Hole Coalescence at Redshift 0.2". In: *Phys. Rev. Lett.* 118.22 (2017). [Erratum: Phys. Rev. Lett.121,no.12,129901(2018)], page 221101. DOI: 10.1103/PhysRevLett.118.221101,10.1103/PhysRevLett.121.129901. arXiv: 1706.01812 [gr-qc].

[120] B. P. Abbott et al. "GW151226: Observation of Gravitational Waves from a 22-Solar-Mass Binary Black Hole Coalescence". In: *Phys. Rev. Lett.* 116.24 (2016), page 241103. DOI: 10.1103/PhysRevLett.116.241103. arXiv: 1606.04855 [gr-qc].

[121] F. Acero. "Detection of Gamma Rays From a Starburst Galaxy". In: *Science* 326 (2009), page 1080. DOI: 10.1126/science.1178826. arXiv: 0909.4651 [astro-ph.HE].

[122] Niklas Karlsson. "Discovery of VHE Gamma-ray Emission from the Starburst Galaxy M82". In: (2009). arXiv: 0912.3807 [astro-ph.HE].

[123] Kohta Murase, Susumu Inoue, and Shigehiro Nagataki. "Cosmic Rays above the Second Knee from Clusters of Galaxies and Associated High-Energy Neutrino Emission". In: *The Astrophysical Journal Letters* 689.2 (2008), page L105. URL: http://stacks.iop.org/1538-4357/689/i=2/a=L105.

[124] U. F. Katz and Ch. Spiering. “High-Energy Neutrino Astrophysics: Status and Perspectives”. In: *Prog. Part. Nucl. Phys.* 67 (2012), pages 651–704. DOI: 10.1016/j.ppnp.2011.12.001. arXiv: 1111.0507 [astro-ph.HE].

[125] Morihiro Honda et al. “Calculation of atmospheric neutrino flux using the interaction model calibrated with atmospheric muon data”. In: *Phys. Rev.* D75 (2007), page 043006. DOI: 10.1103/PhysRevD.75.043006. arXiv: astro-ph/0611418 [astro-ph] (cited on pages 10–12).

[126] M. G. Aartsen et al. “The IceCube Neutrino Observatory - Contributions to ICRC 2017 Part II: Properties of the Atmospheric and Astrophysical Neutrino Flux”. In: (2017). arXiv: 1710.01191 [astro-ph.HE].

[127] Kiyoshi Niu, Eiko Mikumo, and Yasuko Maeda. “A Possible Decay in Flight of a New Type Particle”. In: *Progress of Theoretical Physics* 46.5 (1971), pages 1644–1646. DOI: 10.1143/PTP.46.1644. eprint: /oup/backfile/content_public/journal/ptp/46/5/10.1143/ptp.46.1644/2/46-5-1644.pdf. URL: http://dx.doi.org/10.1143/PTP.46.1644.

[128] Rikard Enberg, Mary Hall Reno, and Ina Sarcevic. “Prompt neutrino fluxes from atmospheric charm”. In: *Phys. Rev.* D78 (2008), page 043005. DOI: 10.1103/PhysRevD.78.043005. arXiv: 0806.0418 [hep-ph] (cited on pages 10–12).

[129] Linyan Wan et al. “Geoneutrinos at Jinping: Flux prediction and oscillation analysis”. In: *Phys. Rev.* D95.5 (2017), page 053001. DOI: 10.1103/PhysRevD.95.053001. arXiv: 1612.00133 [hep-ex].

[130] Kate Scholberg. “Supernova Neutrino Detection”. In: *Ann. Rev. Nucl. Part. Sci.* 62 (2012), pages 81–103. DOI: 10.1146/annurev-nucl-102711-095006. arXiv: 1205.6003 [astro-ph.IM].

[131] Lutz Kopke. “Supernova Neutrino Detection with IceCube”. In: *J. Phys. Conf. Ser.* 309 (2011), page 012029. DOI: 10.1088/1742-6596/309/1/012029. arXiv: 1106.6225 [astro-ph.HE].

[132] C. Grupen. *Astroparticle physics.* 2005. ISBN: 9783540253129. URL: http://www.springer.com/book/3-540-25312-2.

[133] nobel1958. URL: https://www.nobelprize.org/prizes/physics/1958/summary/.

[134] “Design, Implementation and Test of a New Feature Extractor for the IceCube Neutrino Observatory”. In: (2010).

[135] Dmitry Chirkin and Wolfgang Rhode. “Muon Monte Carlo: A High-precision tool for muon propagation through matter”. In: (2004). arXiv: hep-ph/0407075 [hep-ph].

[136] AMANDA collaboration. URL: http://amanda.uci.edu/.

[137] E. Andres et al. “The AMANDA neutrino telescope: Principle of operation and first results”. In: *Astropart. Phys.* 13 (2000), pages 1–20. DOI: 10.1016/S0927-6505(99)00092-4. arXiv: astro-ph/9906203 [astro-ph].

[138] J. Ahrens et al. “Observation of high-energy atmospheric neutrinos with the Antarctic Muon and Neutrino Detector Array”. In: *Phys. Rev.* D66 (2002), page 012005. DOI: 10.1103/PhysRevD.66.012005. arXiv: astro-ph/0205109 [astro-ph].

[139] R. Abbasi et al. “The Design and Performance of IceCube DeepCore”. In: *Astropart. Phys.* 35 (2012), pages 615–624. DOI: 10.1016/j.astropartphys.2012.01.004. arXiv: 1109.6096 [astro-ph.IM].

[140] M. G. Aartsen et al. “Measurement of South Pole ice transparency with the IceCube LED calibration system”. In: *Nucl. Instrum. Meth.* A711 (2013), pages 73–89. DOI: 10.1016/j.nima.2013.01.054. arXiv: 1301.5361 [astro-ph.IM].

[141] M. Ackermann et al. “Optical properties of deep glacial ice at the South Pole”. In: *J. Geophys. Res. Atmos.* 111.D13 (2006), page D13203. DOI: 10.1029/2005JD006687.

[142] Dmitry Chirkin. “Evidence of optical anisotropy of the South Pole ice”. In: *Proceedings, 33rd International Cosmic Ray Conference (ICRC2013): Rio de Janeiro, Brazil, July 2-9, 2013*, page 0580. URL: `http://www.cbpf.br/%7Eicrc2013/papers/icrc2013-0580.pdf`.

[143] M. G. Aartsen et al. “The IceCube Neutrino Observatory: Instrumentation and Online Systems”. In: *JINST* 12.03 (2017), P03012. DOI: `10.1088/1748-0221/12/03/P03012`. arXiv: `1612.05093 [astro-ph.IM]`.

[144] R. Abbasi et al. “Calibration and Characterization of the IceCube Photomultiplier Tube”. In: *Nucl. Instrum. Meth.* A618 (2010), pages 139–152. DOI: `10.1016/j.nima.2010.03.102`. arXiv: `1002.2442 [astro-ph.IM]` (cited on page 16).

[145] M. G. Aartsen et al. “The IceCube Neutrino Observatory - Contributions to ICRC 2017 Part IV: Searches for Beyond the Standard Model Physics”. In: (2017). arXiv: `1710.01197 [astro-ph.HE]`.

[146] M. G. Aartsen et al. “Measurement of the multi-TeV neutrino cross section with IceCube using Earth absorption”. In: *Nature* 551 (2017), pages 596–600. DOI: `10.1038/nature24459`. arXiv: `1711.08119 [hep-ex]`.

[147] M. G. Aartsen et al. “Measurements using the inelasticity distribution of multi-TeV neutrino interactions in IceCube”. In: (2018). arXiv: `1808.07629 [hep-ex]`.

[148] M. G. Aartsen et al. “Searches for Sterile Neutrinos with the IceCube Detector”. In: *Phys. Rev. Lett.* 117.7 (2016), page 071801. DOI: `10.1103/PhysRevLett.117.071801`. arXiv: `1605.01990 [hep-ex]`.

[149] Spencer R. Klein. “Astrophysical Neutrinos with IceCube”. In: *13th Conference on the Intersections of Particle and Nuclear Physics (CIPANP 2018) Palm Springs, California, USA, May 29-June 3, 2018*. 2018. arXiv: `1809.07873 [astro-ph.HE]`.

[150] M. G. Aartsen et al. “A combined maximum-likelihood analysis of the high-energy astrophysical neutrino flux measured with IceCube”. In: *Astrophys. J.* 809.1 (2015), page 98. DOI: `10.1088/0004-637X/809/1/98`. arXiv: `1507.03991 [astro-ph.HE]`.

[151] M. G. Aartsen et al. “Measurement of Atmospheric Neutrino Oscillations at 6–56 GeV with IceCube DeepCore”. In: *Phys. Rev. Lett.* 120.7 (2018), page 071801. DOI: `10.1103/PhysRevLett.120.071801`. arXiv: `1707.07081 [hep-ex]`.

[152] Volker Baum. “Search for Low Energetic Neutrino Signals from Galactic Supernovae and Collisionally Heated Gamma-Ray Bursts with the IceCube Neutrino Observatory”. PhD thesis. Mainz U., Math. Comp. Sci., 2017. URL: `https://publications.ub.uni-mainz.de/theses/frontdoor.php?source_opus=100001660&la=de`.

[153] Thomas Kowarik, Timo Griesel, and Alexander Piegsa. “Supernova Search with the AMANDA / IceCube Detectors”. In: (2009). arXiv: `0908.0441 [astro-ph.HE]`.

[154] Don Colladay and V. Alan Kostelecky. “Lorentz violating extension of the standard model”. In: *Phys. Rev.* D58 (1998), page 116002. DOI: `10.1103/PhysRevD.58.116002`. arXiv: `hep-ph/9809521 [hep-ph]`.

[155] M. G. Aartsen et al. “Neutrino Interferometry for High-Precision Tests of Lorentz Symmetry with IceCube”. In: *Nature Phys.* 14.9 (2018), pages 961–966. DOI: `10.1038/s41567-018-0172-2`. arXiv: `1709.03434 [hep-ex]`.

[156] R. Abbasi et al. “Search for a Lorentz-violating sidereal signal with atmospheric neutrinos in IceCube”. In: *Phys. Rev.* D82 (2010), page 112003. DOI: `10.1103/PhysRevD.82.112003`. arXiv: `1010.4096 [astro-ph.HE]`.

[157] M. G. Aartsen et al. “Search for Neutrinos from Dark Matter Self-Annihilations in the center of the Milky Way with 3 years of IceCube/DeepCore”. In: *Eur. Phys. J.* C77.9 (2017), page 627. DOI: `10.1140/epjc/s10052-017-5213-y`. arXiv: `1705.08103 [hep-ex]`.

[158] M. G. Aartsen et al. "Search for annihilating dark matter in the Sun with 3 years of IceCube data". In: *Eur. Phys. J.* C77.3 (2017), page 146. DOI: 10.1140/epjc/s10052-017-4689-9. arXiv: 1612.05949 [astro-ph.HE].

[159] R. Abbasi et al. "Limits on a muon flux from Kaluza-Klein dark matter annihilations in the Sun from the IceCube 22-string detector". In: *Phys. Rev.* D81 (2010), page 057101. DOI: 10.1103/PhysRevD.81.057101. arXiv: 0910.4480 [astro-ph.CO].

[160] M. G. Aartsen et al. "First search for dark matter annihilations in the Earth with the IceCube Detector". In: *Eur. Phys. J.* C77.2 (2017), page 82. DOI: 10.1140/epjc/s10052-016-4582-y. arXiv: 1609.01492 [astro-ph.HE].

[161] "Quantised singularities in the electromagnetic field," in: *Proceedings of the Royal Society of London A: Mathematical, Physical and Engineering Sciences* 133.821 (1931), pages 60–72. ISSN: 0950-1207. DOI: 10.1098/rspa.1931.0130. eprint: http://rspa.royalsocietypublishing.org/content/133/821/60.full.pdf. URL: http://rspa.royalsocietypublishing.org/content/133/821/60.

[162] G.'t Hooft. "Magnetic monopoles in unified gauge theories". In: *Nuclear Physics B* 79.2 (1974), pages 276–284. ISSN: 0550-3213. DOI: https://doi.org/10.1016/0550-3213(74)90486-6. URL: http://www.sciencedirect.com/science/article/pii/0550321374904866.

[163] Alexander M. Polyakov. "Particle Spectrum in the Quantum Field Theory". In: *JETP Lett.* 20 (1974). [,300(1974)], pages 194–195.

[164] M. G. Aartsen et al. "Search for non-relativistic Magnetic Monopoles with IceCube". In: *Eur. Phys. J.* C74.7 (2014), page 2938. DOI: 10.1140/epjc/s10052-014-2938-8. arXiv: 1402.3460 [astro-ph.CO].

[165] Samridha Kunwar et al. "The IceTop Scintillator Upgrade". In: *PoS* ICRC2017 (2018), page 401. DOI: 10.22323/1.301.0401.

[166] Alexander Aab et al. "The Pierre Auger Observatory Upgrade - Preliminary Design Report". In: (2016). arXiv: 1604.03637 [astro-ph.IM].

[167] Delia Tosi and Hershal Pandya. "Performance of IceTop as a veto for IceCube". In: *PoS* ICRC2017 (2018), page 967. DOI: 10.22323/1.301.0967.

[168] Jan Auffenberg. "IceAct: Imaging Air Cherenkov Telescopes with SiPMs at the South Pole for IceCube-Gen2". In: *PoS* ICRC2017 (2018), page 1055. DOI: 10.22323/1.301.1055.

[169] Satoshi Shimizu et al. "Overview and performance of the D-Egg optical sensor for IceCube-Gen2". In: *PoS* ICRC2017 (2018), page 1051. DOI: 10.22323/1.301.1051.

[170] Lew Classen et al. "The mDOM - A multi-PMT digital optical module for the IceCube-Gen2 neutrino telescope". In: *PoS* ICRC2017 (2018), page 1047. DOI: 10.22323/1.301.1047.

[171] M. Jeong and W. Kang. "A camera system for IceCube-Gen2". In: *PoS* ICRC2017 (2018), page 1040. DOI: 10.22323/1.301.1040.

[172] Elisa Resconi, Kai Krings, and Kai Krings Martin Rongen. "The Precision Optical CAlibration Module for IceCube-Gen2: First Prototype". In: *PoS* ICRC2017 (2018), page 934. DOI: 10.22323/1.301.0934.

[173] Erik Blaufuss, C. Kopper, and C. Haack. "The IceCube-Gen2 High Energy Array". In: *PoS* ICRC2015 (2016), page 1146. DOI: 10.22323/1.236.1146.

[174] Markus Ahlers and Francis Halzen. "Pinpointing Extragalactic Neutrino Sources in Light of Recent IceCube Observations". In: *Phys. Rev.* D90.4 (2014), page 043005. DOI: 10.1103/PhysRevD.90.043005. arXiv: 1406.2160 [astro-ph.HE].

[175] Sebastian Euler, Javier Gonzalez, and Ben Roberts. "Simulation Studies for a Surface Veto Array to Identify Astrophysical Neutrinos at the South Pole". In: *PoS* ICRC2015 (2016), page 1070. DOI: 10.22323/1.236.1070.

[176] Frank G. Schröder. “Radio detection of Cosmic-Ray Air Showers and High-Energy Neutrinos”. In: *Prog. Part. Nucl. Phys.* 93 (2017), pages 1–68. DOI: 10.1016/j.ppnp.2016.12.002. arXiv: 1607.08781 [astro-ph.IM].

[177] P. Allison et al. “Performance of two Askaryan Radio Array stations and first results in the search for ultrahigh energy neutrinos”. In: *Phys. Rev.* D93.8 (2016), page 082003. DOI: 10.1103/PhysRevD.93.082003. arXiv: 1507.08991 [astro-ph.HE].

[178] Christian Glaser. “ARIANNA: Measurement of cosmic rays with a radio neutrino detector in Antarctica”. In: *Acoustic and Radio EeV Neutrino Detection Activities (ARENA 2018) Catania, Italy, June 12-15, 2018*. 2018. arXiv: 1811.10661 [astro-ph.IM].

[179] D Schultz. “IceProd 2: A Next Generation Data Analysis Framework for the IceCube Neutrino Observatory”. In: *Journal of Physics: Conference Series* 664.6 (2015), page 062056. URL: http://stacks.iop.org/1742-6596/664/i=6/a=062056 (cited on page 9).

[180] Giuseppe Battistoni et al. “Overview of the FLUKA code”. In: *Annals Nucl. Energy* 82 (2015), pages 10–18. DOI: 10.1016/j.anucene.2014.11.007 (cited on page 10).

[181] Ralph Engel et al. “Towards the next generation of CORSIKA: A framework for the simulation of particle cascades in astroparticle physics”. In: (2018). arXiv: 1808.08226 [astro-ph.IM] (cited on page 9).

[182] Askhat Gazizov and Marek P. Kowalski. “ANIS: High energy neutrino generator for neutrino telescopes”. In: *Comput. Phys. Commun.* 172 (2005), pages 203–213. DOI: 10.1016/j.cpc.2005.03.113. arXiv: astro-ph/0406439 [astro-ph] (cited on page 10).

[183] M. G. Aartsen et al. “Observation of High-Energy Astrophysical Neutrinos in Three Years of IceCube Data”. In: *Phys. Rev. Lett.* 113 (2014), page 101101. DOI: 10.1103/PhysRevLett.113.101101. arXiv: 1405.5303 [astro-ph.HE] (cited on pages 11, 12).

[184] C. Andreopoulos et al. “The GENIE Neutrino Monte Carlo Generator”. In: *Nucl. Instrum. Meth.* A614 (2010), pages 87–104. DOI: 10.1016/j.nima.2009.12.009. arXiv: 0905.2517 [hep-ph] (cited on page 11).

[185] Costas Andreopoulos et al. “The GENIE Neutrino Monte Carlo Generator: Physics and User Manual”. In: (2015). arXiv: 1510.05494 [hep-ph] (cited on page 11).

[186] M. Honda et al. “Atmospheric neutrino flux calculation using the NRLMSISE-00 atmospheric model”. In: *Phys. Rev.* D92.2 (2015), page 023004. DOI: 10.1103/PhysRevD.92.023004. arXiv: 1502.03916 [astro-ph.HE] (cited on pages 11, 12).

[187] Joerg R. Hoerandel. “On the knee in the energy spectrum of cosmic rays”. In: *Astropart. Phys.* 19 (2003), pages 193–220. DOI: 10.1016/S0927-6505(02)00198-6. arXiv: astro-ph/0210453 [astro-ph] (cited on page 12).

[188] Thomas K. Gaisser. “Spectrum of cosmic-ray nucleons, kaon production, and the atmospheric muon charge ratio”. In: *Astropart. Phys.* 35 (2012), pages 801–806. DOI: 10.1016/j.astropartphys.2012.02.010. arXiv: 1111.6675 [astro-ph.HE] (cited on page 12).

[189] G. D. Barr et al. “Three-dimensional calculation of atmospheric neutrinos”. In: *Phys. Rev. D* 70 (2 July 2004), page 023006. DOI: 10.1103/PhysRevD.70.023006. URL: https://link.aps.org/doi/10.1103/PhysRevD.70.023006 (cited on page 12).

[190] Mario Dunsch et al. “Recent Improvements for the Lepton Propagator PROPOSAL”. In: (2018). arXiv: 1809.07740 [hep-ph] (cited on page 14).

[191] Dmitry Chirkin. “Study of South Pole ice transparency with IceCube flashers”. In: *Proceedings, 32nd International Cosmic Ray Conference (ICRC 2011): Beijing, China, August 11-18, 2011*. Volume 4, page 161. DOI: 10.7529/ICRC2011/V04/0333 (cited on page 15).

[192] Johan Lundberg et al. "Light tracking for glaciers and oceans: Scattering and absorption in heterogeneous media with Photonics". In: *Nucl. Instrum. Meth.* A581 (2007), pages 619–631. DOI: 10.1016/j.nima.2007.07.143. arXiv: astro-ph/0702108 [ASTRO-PH] (cited on page 15).

[193] K. J. Ma et al. "Time and Amplitude of Afterpulse Measured with a Large Size Photomultiplier Tube". In: *Nucl. Instrum. Meth.* A629 (2011), pages 93–100. DOI: 10.1016/j.nima.2010.11.095. arXiv: 0911.5336 [physics.ins-det] (cited on page 16).

[194] J. Ahrens et al. "Muon track reconstruction and data selection techniques in AMANDA". In: *Nucl. Instrum. Meth.* A524 (2004), pages 169–194. DOI: 10.1016/j.nima.2004.01.065. arXiv: astro-ph/0407044 [astro-ph].

[195] M. G. Aartsen et al. "Improvement in Fast Particle Track Reconstruction with Robust Statistics". In: *Nucl. Instrum. Meth.* A736 (2014), pages 143–149. DOI: 10.1016/j.nima.2013.10.074. arXiv: 1308.5501 [astro-ph.IM].

[196] IceCube collaboration. URL: https://internal-apps.icecube.wisc.edu/reports/data/icecube/2014/04/001/icecube_201404001_v1.pdf.

[197] Stef Verpoest. URL: https://lib.ugent.be/fulltxt/RUG01/002/479/620/RUG01-002479620_2018_0001_AC.pdf.

[198] Till Neunhoffer. "Estimating the angular resolution of tracks in neutrino telescopes based on a likelihood analysis". In: *Astropart. Phys.* 25 (2006), pages 220–225. DOI: 10.1016/j.astropartphys.2006.01.002. arXiv: astro-ph/0403367 [astro-ph].

[199] URL: https://wiki.icecube.wisc.edu/index.php/SLC_hit_cleaning.

[200] URL: https://www.dissertations.se/dissertation/fef1f8e4ba/.

[201] Yoav Freund and Robert E Schapire. "A Decision-Theoretic Generalization of On-Line Learning and an Application to Boosting". In: *Journal of Computer and System Sciences* 55.1 (1997), pages 119–139. ISSN: 0022-0000. DOI: https://doi.org/10.1006/jcss.1997.1504. URL: http://www.sciencedirect.com/science/article/pii/S002200009791504X.

[202] S. Fink C. Böser and S. Röcker. *Introduction to boosted decision trees: A multivariate approach to clasification problems*. Presented at the KSETA Doctoral Workshop, Berlin, Germany. July 2014.

Index

V